ANTHROPOLOGY

Modern human incursion into Neanderthal territories 54,000 years ago at Mandrin, France

Ludovic Slimak[1]*†, Clément Zanolli[2]*†, Tom Higham[3,4], Marine Frouin[3,5,6], Jean-Luc Schwenninger[3], Lee J. Arnold[7], Martina Demuro[7], Katerina Douka[4,8], Norbert Mercier[9], Gilles Guérin[10], Hélène Valladas[10], Pascale Yvorra[11], Yves Giraud[11], Andaine Seguin-Orlando[12], Ludovic Orlando[12], Jason E. Lewis[6,13], Xavier Muth[14], Hubert Camus[15], Ségolène Vandevelde[10,16], Mike Buckley[17], Carolina Mallol[18]‡, Chris Stringer[19], Laure Metz[11,20]

Determining the extent of overlap between modern humans and other hominins in Eurasia, such as Neanderthals and Denisovans, is fundamental to understanding the nature of their interactions and what led to the disappearance of archaic hominins. Apart from a possible sporadic pulse recorded in Greece during the Middle Pleistocene, the first settlements of modern humans in Europe have been constrained to ~45,000 to 43,000 years ago. Here, we report hominin fossils from Grotte Mandrin in France that reveal the earliest known presence of modern humans in Europe between 56,800 and 51,700 years ago. This early modern human incursion in the Rhône Valley is associated with technologies unknown in any industry of that age outside Africa or the Levant. Mandrin documents the first alternating occupation of Neanderthals and modern humans, with a modern human fossil and associated Neronian lithic industry found stratigraphically between layers containing Neanderthal remains associated with Mousterian industries.

INTRODUCTION

Homo sapiens emerged in Africa over 300 thousand years (ka) ago (*1*, *2*), and anatomically modern humans by at least 195 ka ago (*3*). The first pulses of early modern humans outside Africa are found in Israel at ~194 ka to 177 ka ago (*3*) and possibly Greece by ~210 ka ago (*4*). The Levant is traditionally thought to have played a fundamental role in the dispersal of modern humans, but the Late Pleistocene paleoanthropological record from this region is patchy (*5*, *6*). Modern human remains are documented in East Asia as early as ~80 ka ago (*7*), and from archeological evidence, modern humans reached Australia by ~65 ka ago (*8*). In Europe, however, their appearance seems to have occurred much later, perhaps because of ecological barriers and/or the occupation of the region by Neanderthals (*5*). The earliest evidence of Late Pleistocene *H. sapiens* settlement in Europe is constrained to ~45 ka to 43 ka ago based on five isolated dental remains from three Italian sites [Grotta Cavallo in Southern Apulia, Riparo Bombrini in the western Ligurian Alps, and Grotta di Fumane in the western Lessini Mountains (*9*–*12*)] and Bacho Kiro in Bulgaria (*13*). The latest Neanderthal remains in Europe are dated to 42 ka to 40 ka ago (*14*–*16*), while their Mousterian technologies ended by ~41 ka to 39 ka ago (*16*). In this period, Mousterian technologies are commonly stratigraphically replaced by so-called transitional industries (e.g., Uluzzian, Châtelperronian, and Bohunician) (*5*, *9*, *11*, *12*, *16*–*18*), for whom the taxonomic identity of the maker remains intensely debated (*5*, *9*–*12*, *14*, *19*). These are followed by the Protoaurignacian and Early Aurignacian, considered to be the archeological signature of modern humans (*5*, *10*, *20*, *21*). The records show that the earliest modern human remains and all transitional industries are systematically found stratigraphically above, and so after, Middle Paleolithic/Neanderthal levels (*5*, *9*–*13*, *16*, *20*–*24*), making it impossible to demonstrate any likely encounter between the two populations in any particular region of Europe. Here, we report hominin fossils found in Grotte Mandrin, Mediterranean France, that reveal the earliest known arrival of modern humans in Europe, between

[1]CNRS, UMR 5608, TRACES, Université de Toulouse Jean Jaurès, 5 Allées Antonio Machado, 31058 Toulouse Cedex 9, France. [2]Université de Bordeaux, CNRS, MCC, PACEA, UMR 5199, 33600 Pessac, France. [3]Research Laboratory for Archaeology and the History of Art, University of Oxford, Dyson Perrins Building, South Parks Road, Oxford OX1 3QY, UK. [4]Department of Evolutionary Anthropology, University of Vienna, University Biology Building, Djerassiplatz 1, A-1030 Vienna, Austria. [5]Department of Geosciences, Stony Brook University, 255 Earth and Space Sciences Building, Stony Brook, NY 11794-2100, USA. [6]Turkana Basin Institute, Stony Brook University, Stony Brook, NY 11794-4364, USA. [7]School of Physical Sciences, Environment Institute, Institute for Photonics and Advanced Sensing (IPAS), University of Adelaide, North Terrace Campus, Adelaide, SA 5005, Australia. [8]Department of Archaeology, Max Planck Institute for the Science of Human History, Kahlaische, Str. 10, 07745 Jena, Germany. [9]CNRS, UMR 5060, Institut de Recherche sur les Archéomatériaux and Centre de Recherche en Physique Appliquée à l'Archéologie (CRP2A), Maison de l'Archéologie, Université Bordeaux Montaigne, 33607 Pessac, France. [10]Laboratoire des Sciences du Climat et de l'Environnement, LSCE/IPSL, UMR 8212 CEA CNRS UVSQ, Université Paris-Saclay, 91191 Gif-sur-Yvette, France. [11]Aix-Marseille Université, CNRS, Min. Culture, UMR 7269, LAMPEA, Maison Méditerranéenne des Sciences de l'Homme, BP 647, 5 rue du Château de l'Horloge, F-13094, Aix-en-Provence Cedex 2, France. [12]CNRS, UMR 5288, CAGT, Université Toulouse III Paul Sabatier, Toulouse, France. [13]Department of Anthropology, Stony Brook University, Stony Brook, NY 11794-4364, USA. [14]Get in Situ, CH1097 Riex, Switzerland. [15]PROTEE-EXPERT, 4 rue des Aspholdèles, 34750 Villeneuve-lès-Maguelone, France. [16]Université Paris 1–Panthéon-Sorbonne, Équipe Archéologies Environnementales, UMR 7041, ArScAn, Équipe Archéologies Environnementales, 21 allée de l'Université, 92023 Nanterre Cedex, France. [17]Department of Earth and Environmental Sciences, University of Manchester, Oxford Road, Manchester M13 9PL, UK. [18]Archaeological Micromorphology and Biomarkers Laboratory (AMBI Lab), Instituto Universitario de Bio-Orgánica Antonio González, Departamento de Geografía e Historia, UDI Prehistoria, Arqueología e Historia Antigua, Facultad de Geografía e Historia, Universidad de La Laguna, Tenerife, Spain. [19]Centre for Human Evolution Research (CHER), Department of Earth Sciences, Natural History Museum, London SW7 5BD, UK. [20]College of Liberal Arts and Sciences, University of Connecticut, 215 Glenbrook Road, U-4098, Storrs, CT 06269-4098, USA.
*Corresponding author. Email: slimak@univ-tlse2.fr (L.S.); clement.zanolli@gmail.com (C.Z.)
†These authors contributed equally to this work.
‡Present address: ICArEHB–Interdisciplinary Center for Archaeology and the Evolution of Human Behaviour FCHS, Campus de Gambelas, Universidade do Algarve, 8005-139 Faro, Portugal.

56,800 and 51,700 calibrated years before the present (cal. B.P.). We demonstrate successive replacement phases in occupation at the site—Neanderthals/modern humans/Neanderthals/modern humans—over the last millennia of Neanderthals' existence. Last, we identify important technical differences in the lithic industries within the archeological sequence that we can directly associate with the two different human groups.

Grotte Mandrin, located near the town of Malataverne, overlooks the eastern bank of the middle Rhône River Valley at an elevation of 225 m (Fig. 1). Since 1990, excavations have revealed a 3-m deep

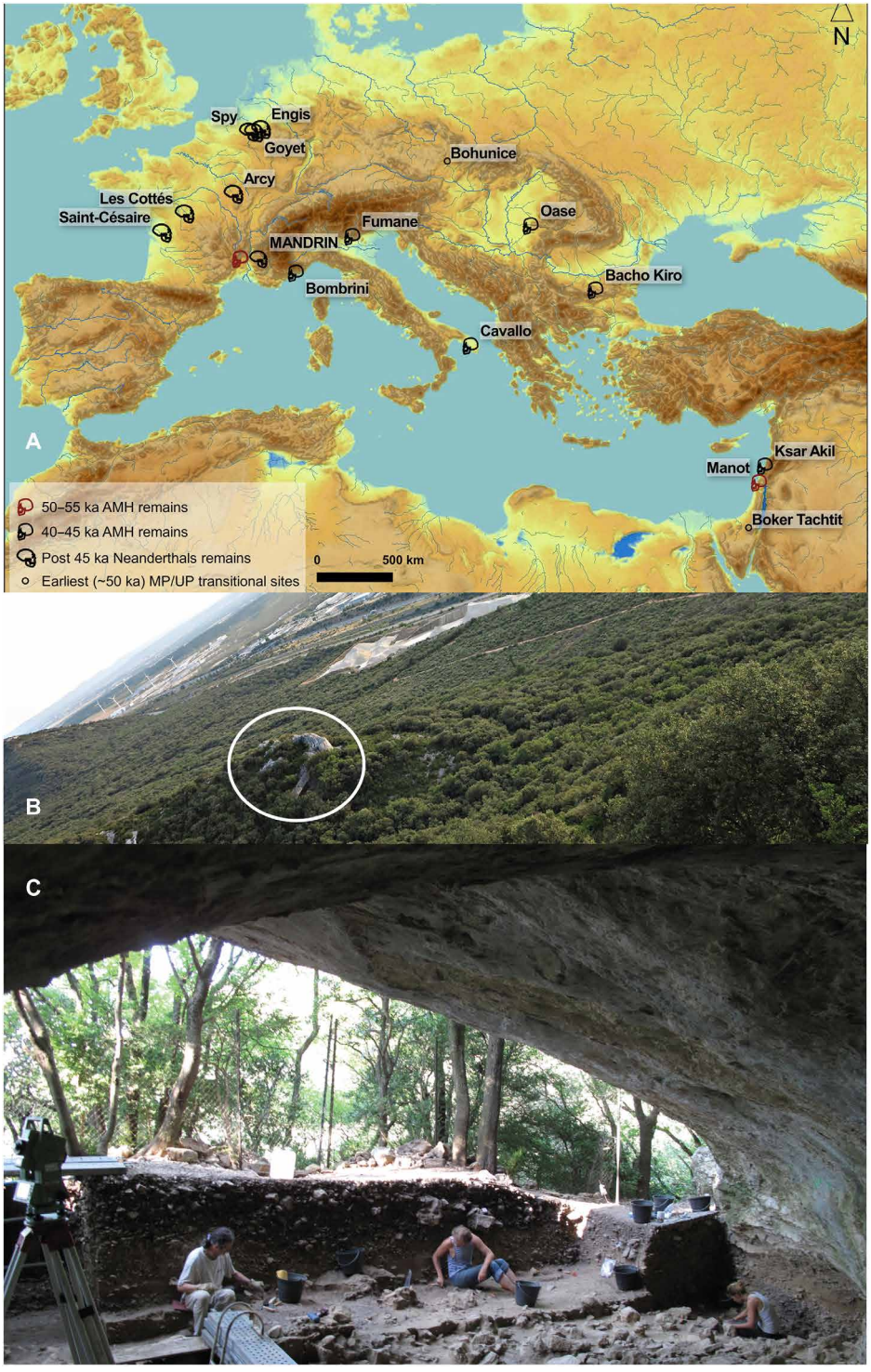

Fig. 1. Grotte Mandrin. (**A**) Geographic location and other sites mentioned in the text. (**B**) Situation of the rockshelter overlooking the Rhône River Valley. (**C**) View looking out from the back of the shelter. AMH, anatomically modern human; MP, middle paleolithic; UP, upper paleolithic. Photo credit: Ludovic Slimak, CNRS.

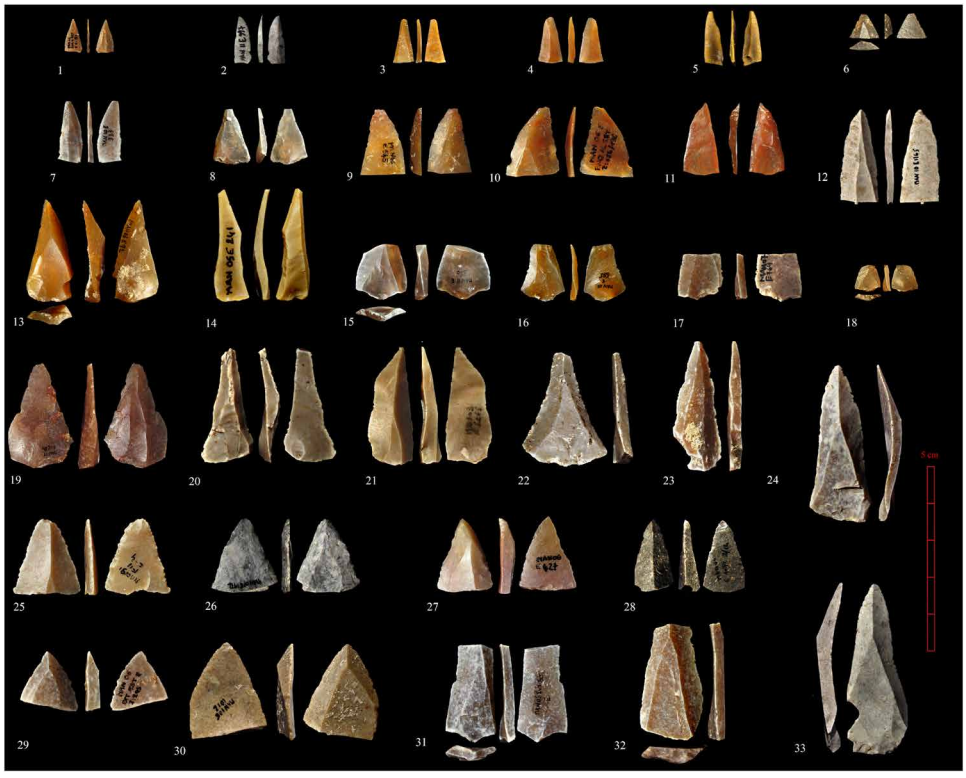

Fig. 2. Neronian points from Mandrin layer E. Micro- and nanopoints (numbers 1 to 23), pointed micropoint (number 10), and points (numbers 24 to 33).

stratigraphic sequence containing 12 archeological layers (layers J to B1) ranging from marine isotope stage (MIS) 5 to the very end of the Middle Paleolithic, and the emergence of the Upper Paleolithic [fig. S1, A and B (*20*, *25*–*27*)]. These layers are within a sedimentary deposit comprising local clay at the base (layers J to G), eolian sand in the middle (layers F to D), and coarse roof spall at the top (layers C and B). The entire sequence is particularly well preserved as shown by geological, spatial, and microstratigraphic analyses (figs. S2 to S4) and by a rich corpus of direct ages from all layers that reveal no major outliers in the sequence (notes S1 to S4). The site has yielded a rich and well-preserved archeological collection, including nearly 60,000 lithic objects (Figs. 2 to 4 and figs. S5 and S6) and more than 70,000 faunal remains dominated by horse, bison, and deer. In particular, layer E contains a remarkable industry characterized by standardized small points (see note S3), some measuring only 1 cm in length. These points represent a substantial technological difference from all of the Mousterian industries in the Mandrin sequence (Fig. 2, table S11, and note S3) (*20*, *25*, *27*). Because of the distinct features of this assemblage and other similar ones from penecontemporaneous levels at nearby sites, they were given a unique cultural attribution: the "Neronian" [after the Grotte de Néron site; figs. S7 to S10 (*20*, *25*, *26*)]. Until now, the Neronian industry had not been documented anywhere as early as at Mandrin (note S5), and its makers had not been identified.

RESULTS

Hominin remains

Hominin fossils, comprising nine dental specimens, have been found in situ in most of Mandrin's layers (Fig. 5 and fig. S11) representing a minimum of seven individuals (Table 1 and note S6). Ancient DNA analyses were initially carried out on fossil horse material excavated from throughout the stratigraphic sequence to assess the level of DNA preservation, and whether destructive attempts to recover DNA from the hominin remains to identify the population affiliation of these individuals would be warranted (see Materials and Methods and table S12). However, the overall poor preservation signal from the horse material cautioned against sampling hominin remains at this time (note S7).

We therefore investigated the structural morphology of dental elements from layers G to C, with special attention paid to the single specimen from layer E: a deciduous maxillary second molar crown (Udm2; Man12 E 1300). By combining the study of dental metric and nonmetric features with shape analyses of the crown outline (for the most worn specimens) and the enamel-dentine junction (EDJ; for the specimens only moderately affected by occlusal wear), assessment of enamel thickness, and root proportions (note S6 and tables S13 to S19), it is possible to distinguish Neanderthals and modern humans (*10*, *11*). In the EDJ shape analysis of the permanent lower first molar (LM1; Fig. 6), Neanderthals on the one hand and Upper Pleistocene and Holocene modern humans on the other tend to be discriminated along between-group principal component 1 (bgPC1) (representing 60.02% of the total variance). Neanderthal EDJs show higher topography and more centrally placed dentine horn tips than in modern humans. No allometric signal is detected along this axis ($P = 0.16$; $R^2 = 0.07$). The three dentine horn tip reconstructions (see Materials and Methods) of layer F permanent LM1 Man98 F 811 fall within the Neanderthal range of variation. Similarly, the outline analyses of the deciduous upper second molars from layer D

Fig. 3. Mandrin layer E and layer D lithic industries. (**A**) Layer D post–Neronian I Mousterian. Pseudo-Levallois points with truncated back in black exotic flints coming from ~70 to 90 km northeast of the site. (**B**) Mandrin layer E Neronian. Blades, bladelets, and bladelets by-products. Numbers 1 to 21, bladelets; number 18, crested bladelet; number 22, blade.

(Udm2; Fig. 6) and lower second molar from layer C (Ldm2; Fig. 6), respectively, partially and fully separate Neanderthals and Upper Pleistocene to Holocene modern humans along bgPC1 (88.70 and 96.94%, respectively). For the Udm2, bgPC1 is characterized by size-independent shape variation ($P = 0.09$; $R^2 = 0.07$), while for the Ldm2, slight allometric influence is noted along the first axis ($P < 0.01$; $R^2 = 0.26$). The Udm2 Man04 D 395 and Man04 D 679 from layer D and the Ldm2 Man11 C 204 from layer C plot with the Neanderthals. Our results identify all the specimens found in layers D, C, F, and G as belonging to Neanderthals (Fig. 6, figs. S12 to S14, tables S15 to S22, and note S6). The EDJ analysis of the Udm2 Man12 E 1300 from layer E, however, shows a different signal (Fig. 6). bgPC1 (85.53%) distinguishes between Neanderthal and Upper Pleistocene to Holocene humans, showing some size-dependent variation in addition to shape differences ($P < 0.01$; $R^2 = 0.31$). The three reconstructions of the dentine horn tips (see Materials and Methods and fig. S13) cluster together, unambiguously falling with Upper Pleistocene modern humans and not with Holocene humans, and are outside

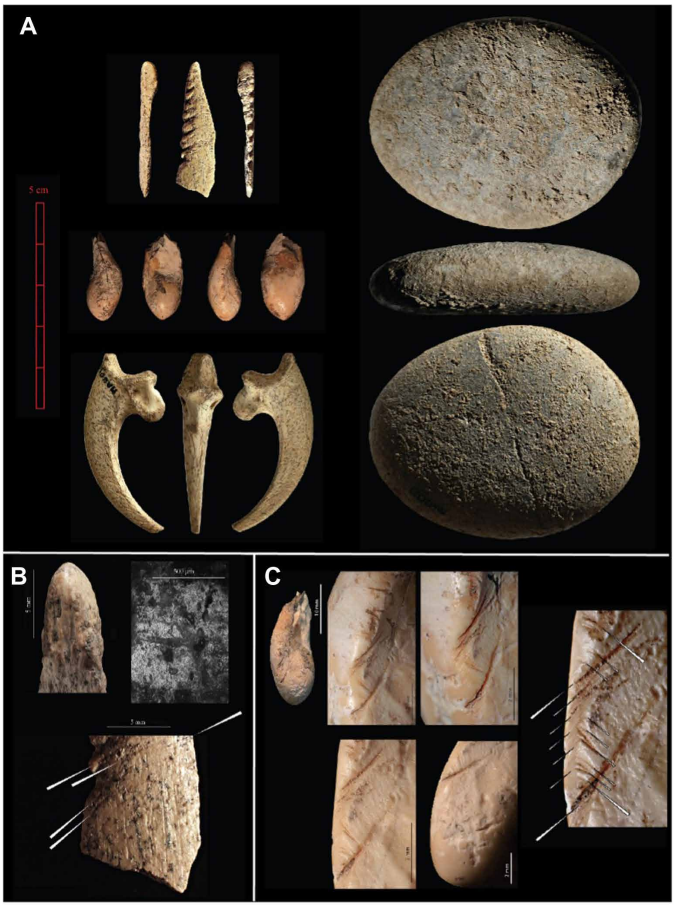

Fig. 4. Neronian artifacts from layer E. (**A**) Top to Bottom: Pointed bone point with lateral notches, worked red deer canine, eagle talon with cutmarks, and pebble with an engraved line separating the rock in two subequal parts. (**B**) Details of the bone point showing working traces by a flint tool. (**C**) Red deer canine details showing traces of scrapping by a lithic tool. These marks may have been to deliberately extract the canine or to modify its morphology.

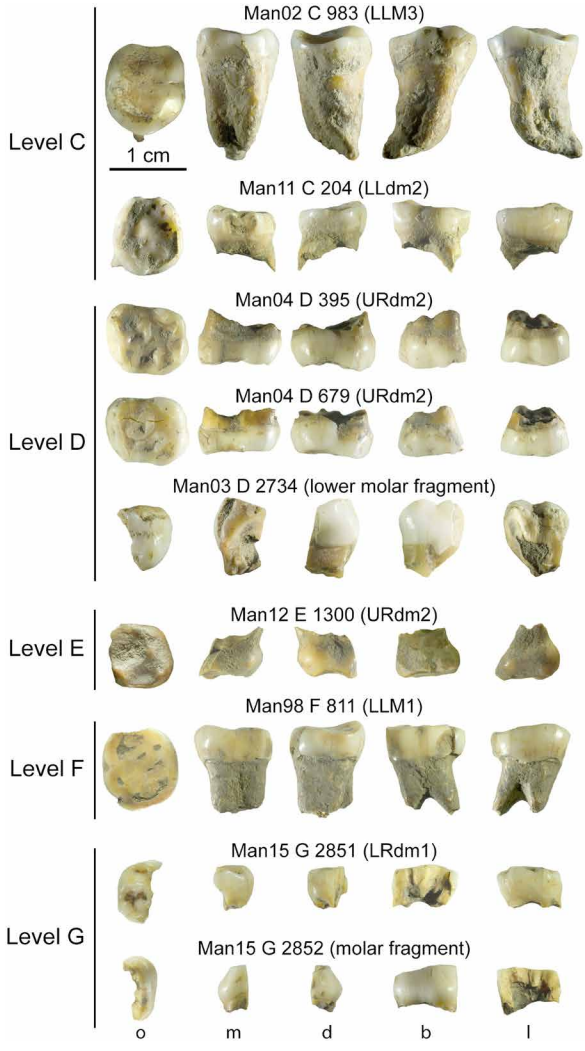

Fig. 5. The Grotte Mandrin human remains. Plate illustrating the nine dental elements preserved in layers G to C (see note S5 for a detailed description of the fossil human remains). LLdm2, deciduous lower left second molar; LLM1, permanent lower left first molar; LRM3, permanent lower right third molar; URdm2, deciduous upper right second molar; b, buccal; d, distal; l, lingual; m, mesial; o, occlusal.

the variation of Neanderthals along bgPC2 (Figs. 6 and 7). Even when restricting the geometric morphometric analysis of the Udm2 EDJ to the talon portion, both two-dimensional (2D) analysis (that does not necessitate any reconstruction) and 3D analysis of the reconstructions of Man12 E 1300 fall with Late Pleistocene modern humans and are discriminated from Neanderthals (Fig. 7). The cross-validated bgPCA results are supported by the canonical variate analysis (CVA) analyses in which the teeth from layers F, D, and C are classified as Neanderthals and the Man12 E 1300 specimen from layer E is unequivocally classified as an Upper Pleistocene modern human (tables S20 to S22).

Dating

To constrain the chronology of the site, we obtained high-quality accelerator mass spectrometry (AMS) radiocarbon ages from the University of Oxford Radiocarbon Accelerator Unit (ORAU) and luminescence ages from throughout the sequence at the University of Oxford Luminescence Laboratory, the University of Adelaide laboratory, and, for the base of the sequence, at the Laboratoire des Sciences du Climat et de l'Environnement (see Materials and Methods). We built a Bayesian model integrating all of the ages in combination with the geo archeological sequence information (Fig. 8 and table S3). We determined that layer E, which contains the modern human fossil, dates to 56.8 ka to 51.7 ka cal. B.P. (95.4% prob.; see Materials and Methods; figs. S15 to S20 and tables S1 to S10), suggesting that this individual is substantially earlier than any previously documented modern human remains or potential transitional archeological assemblages in Europe, and penecontemporaneous with, if not older than, the Manot 1 calvaria from Israel (*6*).

Lithics

Neronian industries have been identified in four other sites from the middle Rhône Valley: Néron, Figuier, Moula, and Maras (*25*), and were initially termed "evolved Mousterian" (*26*). Unfortunately, these sites were mainly excavated between 1869 and 1950, and their Neronian layers provided few lithics, appearing mixed with Mousterian industries [figs. S7 to S10 and note S3 (*20*, *25*, *26*, *28*, *29*)]. Evidence from

Table 1. List of the Grotte Mandrin hominin specimens. LLdm2, deciduous lower left second molar; LLM1, permanent lower left first molar; LRM3, permanent lower right third molar; URdm2, deciduous upper right second molar.

Specimens	Stratigraphic position	Anatomical part	Age	Individual attribution
Man02 C 983	Layer C	LRM3	Adult	Individual 1
Man11 C 204	Layer C	LLdm2	Juvenile	Individual 2
Man04 D 395	Layer D	URdm2	Juvenile	Individual 3
Man04 D 679	Layer D	URdm2	Juvenile	Individual 4
Man03 D 2734	Layer D	Deciduous or permanent lower molar fragment	Indet.	*
Man12 E 1300	Layer E	URdm2	Juvenile	Individual 5
Man98 F 811	Layer F	LLM1	Adult	Individual 6
Man15 G 2851	Layer G	LRdm1	Juvenile	Individual 7
Man15 G 2852	Layer G	Deciduous molar fragment	Juvenile	*

*The fragmentary state of these specimens makes it difficult to give them a secure metameric position attribution, and it is thus not possible to ascertain if they belong to one of the other individuals found in the same stratigraphic layer. For these reasons, we parsimoniously leave these fragmentary specimens unattributed to any of the individuals and assess the minimum number of individuals in the assemblage to seven.

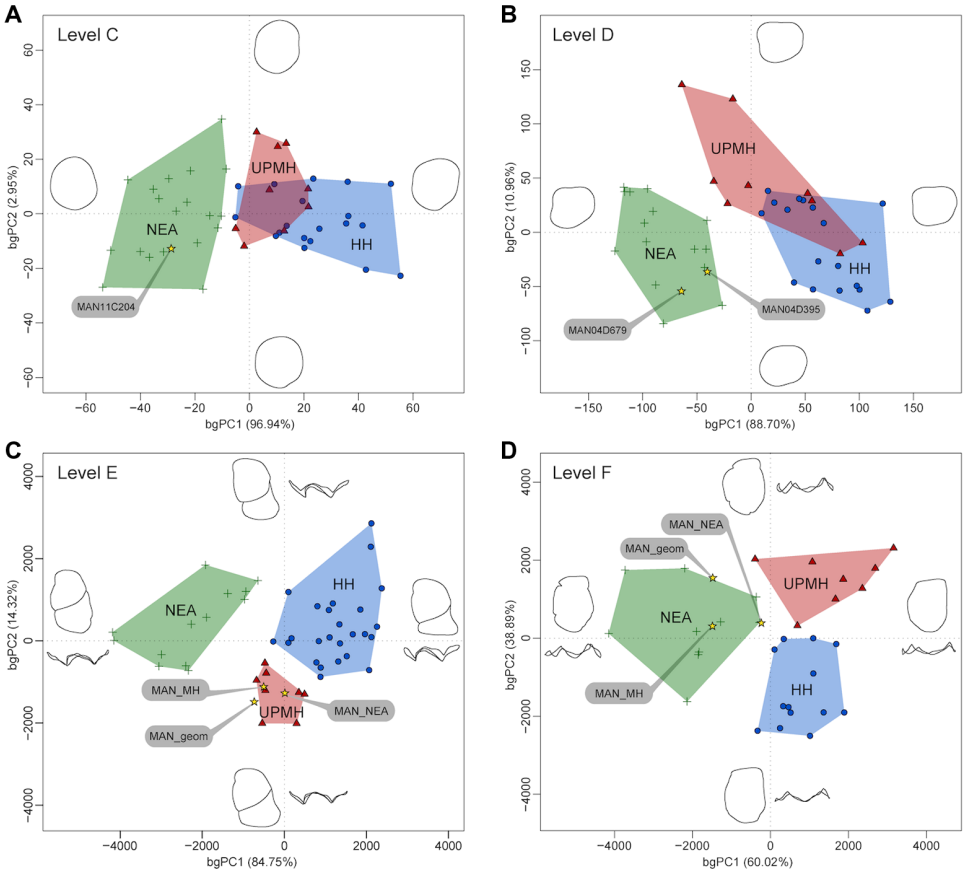

Fig. 6. Geometric morphometric analyses of the crown outline and EDJ shape. (**A** and **B**) Between-group principal components analyses (bgPCA) based on the two-dimensional (2D) landmarks Procrustes-registered shape coordinates of the crown outline of the deciduous lower second molar (Ldm2) Man11 C 204 from layer C (A) and of the deciduous upper second molars (Udm2) Man04 D 395 and Man04 D 679 from layer D (B) compared with fossil and extant hominins. (**C** and **D**) bgPCA based on the 3D landmarks Procrustes-registered shape coordinates of the enamel-dentine junction reconstructions of the Udm2 Man12 E 1300 from layer E (C) and of the permanent lower first molar (LM1) Man98 F 811 from layer F (D) compared with fossil and extant hominins. NEA, Neanderthals; UPMH, Upper Pleistocene modern humans; HH, Holocene humans; MAN_geom, geometric-based reconstruction of the Mandrin specimens; MAN_MH, modern human-based reconstruction of the Mandrin specimens; MAN_NEA, Neanderthal-based reconstruction of the Mandrin specimens (table S14).

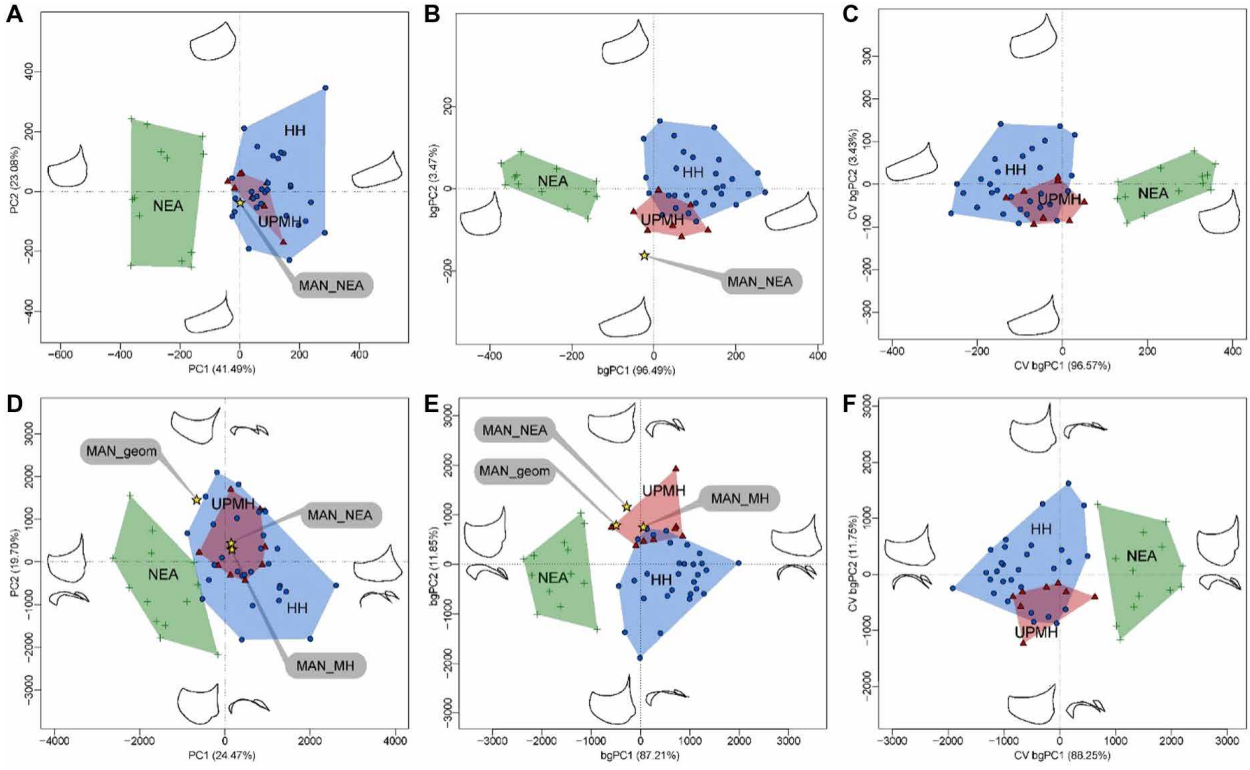

Fig. 7. Geometric morphometric analyses of the talon of the Udm2 EDJ. (**A**) PCA based on the 2D landmarks Procrustes-registered shape coordinates of the EDJ talon shape of the Udm2 Man12 E 1300 and of the comparative fossil and extant hominin groups. (**B** and **C**) bgPCA (B) and cross-validated bgPCA (C) based on the same data. (**D**) PCA based on the 3D landmarks Procrustes-registered shape coordinates of the EDJ talon shape of the three reconstructions of the Udm2 Man12 E 1300 and of the comparative fossil and extant hominin groups. (**E** and **F**) bgPCA (E) and cross-validated bgPCA (F) based on the same data (table S14).

Mandrin layer E and comparisons with other penecontemporaneous assemblages allow a fuller understanding of this cultural system. In the Neronian, blades and points are produced from the same technical system, with two schemas that can be recognized: a blade/point and a bladelet/micropoint schema (*25*). The first phase of flaking is then focused on the making of blades or bladelets before the extraction of well-standardized points (Figs. 2 and 3). The production sequence is initiated with crested blades/bladelets. Blades and points were the exclusive end products of this technology (*25*). Thin ventral convergent retouch transformed some of these tools into a Soyons Point, a classic typological category of these industries (*25*, *26*). The Neronian industries illustrate a remarkable technical precision in their execution (*25*). They are characterized by a noticeable proportion of standardized micropoints (*25*) showing a maximum length of 3 cm for a third of the end products. Tiny points, called nanopoints, can be less than 10 mm in maximum length. Use-wear analyses show that these microliths were mainly used with no secondary modifications (*25*).

The presence of all production phases, from initiation to the abandonment of the products, shows that the full production process was carried out in the shelter. The Mandrin E lithics were produced from particularly homogeneous raw material blocks of superior quality as compared to the other units of the sequence. This differential selection can in part be attributed to the production systems that require employment of rocks of great homogeneity. Raw material sourcing analysis indicates that the layer E humans had a large territorial influence, since almost half of the rocks (46.6%) come from a very large area, where the nearest rocks come from 15 to 35 km (Meysse-Rochemaure) and up to 60 to 90 km away (*20*, *25*).

Although Levallois point technologies are rare in the Middle Paleolithic of Europe, they are common in the eastern Mediterranean area, and it was recently proposed that Mandrin E shared precise technical features with the Initial Upper Paleolithic (IUP) in the Levantine region (notes S3 and S5) (*20*). Direct technical comparisons with lithic artifacts from levels XXV to XX at Ksar Akil, Lebanon (stored at Harvard University's Peabody Museum of Archaeology and Ethnology) and dating to >44.6 ka to 41.6 ka ago (*30*) and ~43 ka to 39 ka ago (*31*) show that the Neronian industry bears notable technical similarities with the IUP there (fig. S21). The technologies used to produce the points from both the Ksar Akil IUP and the Neronian are the same, and a comparison of the tip cross-sectional area (the ratio of width/thickness) of points from both sites shows no statistically significant difference (Fig. 9). The beginning of the IUP in the Levant, represented in level 1 at Boker Tachtit (*32*), is slightly younger than the Neronian in Mandrin (see Materials and Methods and fig. S20). The IUP industries at Ksar Akil are followed by technically close industries assigned to the Early Upper Paleolithic [EUP; layers XIX to XIV (*33*, *34*)], and it has been demonstrated that the EUP is technically a direct descendant of the local IUP (*20*, *30*–*36*). A juvenile modern human and a modern human upper jaw were recovered from the EUP and IUP layers of Ksar Akil, respectively, and therefore, most scholars accept that both the IUP and EUP there were made by *H. sapiens* (*20*, *31*, *37*). The similarities between Mandrin E and Ksar Akil suggest that members of the IUP populations spread very early through

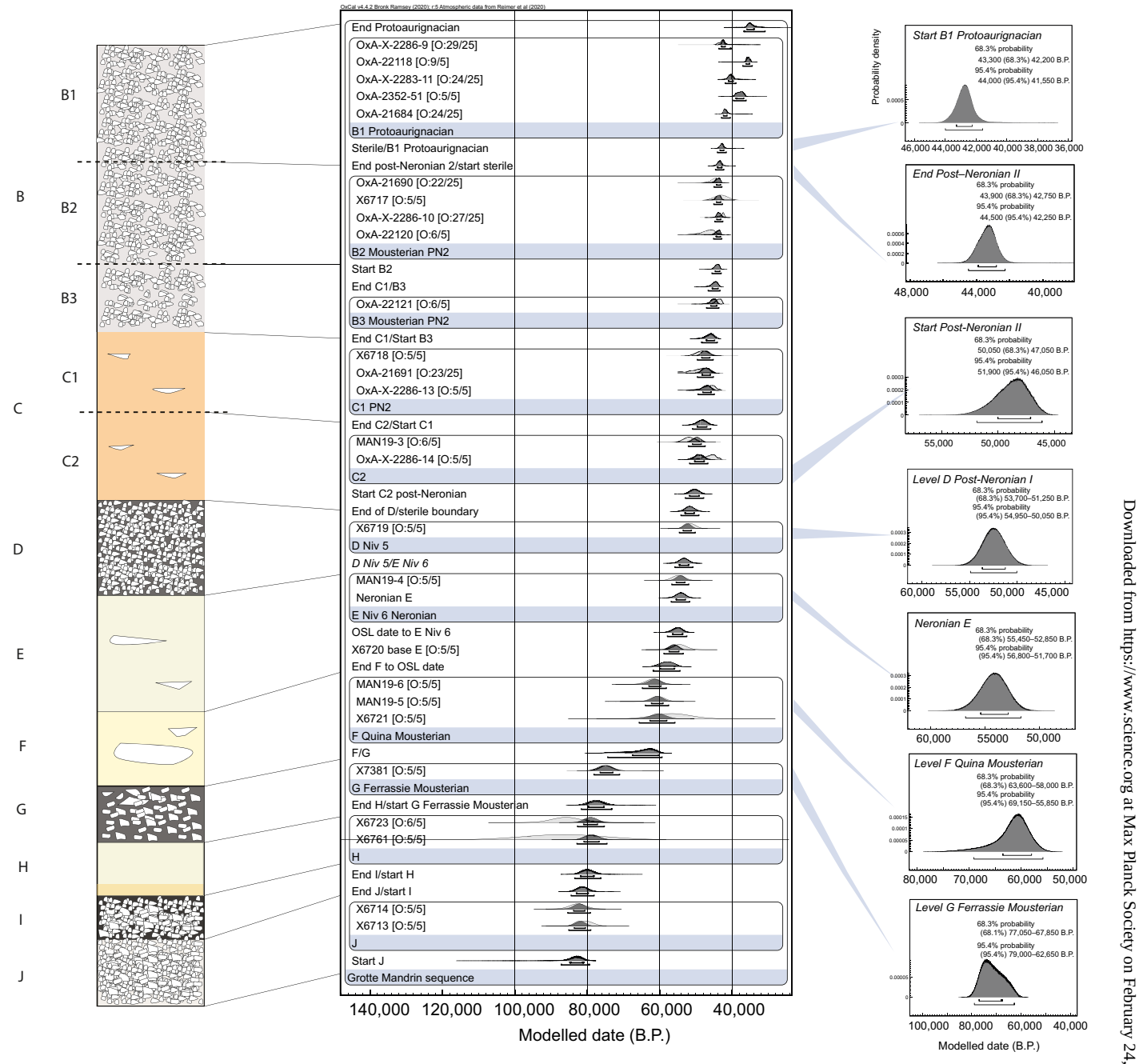

Fig. 8. The Grotte Mandrin Bayesian model. The model comprises the radiocarbon likelihoods and optically stimulated luminescence ages fitted within a relative age sequence that is based on the succession of archeological levels excavated at the site. A composite stratigraphy is shown at the left illustrating these stratigraphic horizons. Key probability distributions from the Bayesian model are shown on the right. These are either Boundary distributions (the top three) representing the start of a Phase, or Date ranges (the lower four) that represent the age spans of an archeological phase.

the Mediterranean basin, pushing back the earliest appearance of the Upper Paleolithic in Western Europe by ~12 ka ago and all of continental Europe by ~10 ka ago.

DISCUSSION

Previous consensus in paleoanthropology held that settlements of modern humans in Europe around 45 to 40 ka cal. B.P. coincided with the demise of Neanderthals shortly thereafter (*5*, *9*–*21*). Multiple episodes of interbreeding between modern humans and Neanderthals likely occurred in Asia (*38*–*44*), and current paleogenetic data show that ancient gene flow between these groups may have also, to some degree, occurred in Europe (*45*), although no genetic traces have been detected so far among the last representatives of the Neanderthal population (*46*).

The archeological and fossil evidence described here from layer E at Mandrin documents an incursion of modern humans into Europe

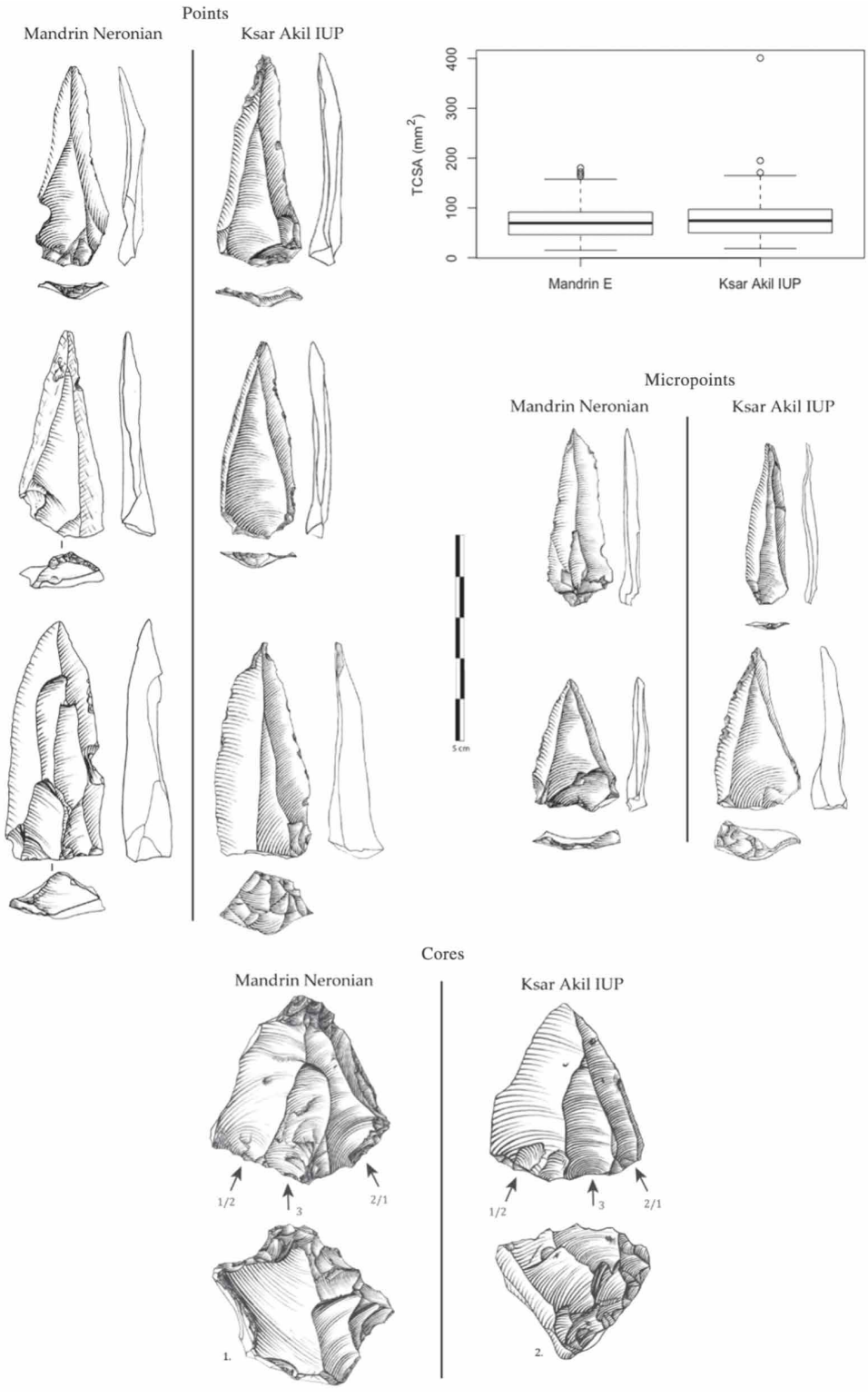

Fig. 9. Neronian (Mandrin layer E) and Initial Upper Paleolithic points, micropoints and cores (Ksar Akil layers XXV-XX, Lebanon, Peabody Museum collections). Drawings L. Metz. These points are precisely obtained through the same technical processes and show identical morphologies. Boxplot in upper right shows that their metrics (tip cross-sectional area; ratio width/thickness and statistic comparisons between Mandrin E points and Ksar Akil IUP points; measures at 1-mm precision) are also identical (Wilcox test: $w = 4156$; $P = 0.1883$, $P > 0.01$).

~10 millennia earlier than previously identified, by groups that appear to have had major technological advantages over contemporaneous Neanderthal groups (*27*). The rich and well-preserved Neronian industry in layer E, which we directly link with *H. sapiens*, had previously been regarded as a technological anomaly because of its distinctive features and intercalation between classic Neanderthal Mousterian layers (Figs. 2 to 4, figs. S5, S6, and S22, and note S3) (*20*, *25*). Mandrin reveals an unexpectedly complex process of hominin successions in the middle Rhône Valley, the most important natural corridor linking the Mediterranean Basin with the Northern European steppes. The geographical location of the site, overhanging the second most important river input to the Mediterranean Sea, represents a key for understanding these hominin successions at the Mediterranean basin scale. Modern humans are documented in the Levantine area by 54.7 ± 5.5 ka (*6*), but before the current study, there was nearly a 10-ka gap before comparable records appear in Europe at Bacho Kiro (*13*) or at Italian sites along the coast or near rivers (*9*–*12*). Together, these data suggest that the Mediterranean basin, from the Levantine coast to the Rhodanian corridor, appears to have played a major role during the geographic expansion of modern humans in Western Eurasia.

The results from Grotte Mandrin presented here show that instead of recording a single event of population replacement as often argued elsewhere in Europe, a much more complex process of modern human appearance and Neanderthal disappearance appears to have occurred in Western Europe. We document at least four alternating phases of replacement, with Neanderthals occupying the area around Mandrin from MIS 5 up to ~54 ka cal. B.P. (Mandrin layers J to F), a modern human incursion at around 54 ka cal. B.P. (56.8 to 51.7 ka cal. B.P.; Mandrin E) followed by Neanderthal reoccupations (Mandrin D-C2-C1-B3-B2), and a second modern human phase from ~44.1 ka to 41.5 ka cal. B.P. (Mandrin B1) onward. Apart from Mandrin, only the archeological sequence at Buran Kaya III in Crimea is known to record a stratigraphic replacement of transitional industries by Middle Paleolithic industries. However, it lacks hominin remains in the relevant layers (*23*).

A high-resolution geochronological approach has shown that the duration between the last occupation of Neanderthals from layer F from and the first occupation of *H. sapiens* from layer E was short, estimated to be around a year [figs. S23 to S25 and note S8; (*47*, *48*)], a scenario compatible with the Bayesian model age estimates for layers F and E that overlap and cannot be statistically separated. The Mandrin succession represents the first record of plausible penecontemporaneity of Neanderthals and modern humans in a geographically defined area in Europe. Such a rapid succession highlights the remarkable technological divergences existing between the coeval hominins in this region. This succession also represents the first known archeological evidence in Europe for the interstratification of a modern human occupation between those of Neanderthals (Mandrin E versus Mandrin F and Mandrin D). Analyses of the abundant preceding (Mandrin F) and succeeding (Mandrin D to B2) lithic industries reveal no obvious processes of cultural exchange in terms of technical traditions either between the different Neanderthal groups or between modern human and Neanderthal populations (*20*, *25*), a situation congruent with a scenario of rapid replacement processes with no major interactions. These data illustrate that the replacement of indigenous Neanderthal groups was not a straightforward single event but a complex historical process during which both populations replaced each other rapidly or even abruptly, at least twice, in the same territory.

MATERIALS AND METHODS

Hominin fossil analyses

All the hominin specimens coming from layers F to C at Mandrin were scanned using x-ray microtomography (X-µCT). The X-µCT data were processed in Avizo 8.0 (FEI Visualization Sciences Group), and 2D and 3D analyses were conducted, including comparisons of mesiodistal and buccolingual diameters, 3D lateral crown tissue proportions (i.e., lateral average enamel thickness and lateral relative enamel thickness), 3D root proportions (i.e., root stem volume versus root branch volume), and both 2D and 3D geometric morphometric analyses of the occlusal crown outline and EDJ shape. A combination of statistical analyses was used to assign the Mandrin teeth to a taxon (Neanderthal versus modern human), including adjusted *z* scores, between-group principal components analyses (normal and cross-validated), and canonical variate analyses (normal and cross-validated). More details on methodological aspects can be found in the Supplementary Materials and Methods.

Radiocarbon dating

Radiocarbon and chemical pretreatment methods

Radiocarbon samples for this paper were AMS dated at the ORAU, University of Oxford, after careful selection of samples at the site and postexcavation collections. All of the radiocarbon samples selected for dating from the Grotte Mandrin were bones. Only artifacts and humanly modified bones were sampled. Several retouchers (*retouchoirs*) were directly dated, particularly from the lower layers of the site. Bone from these objects was very carefully sampled to preserve the key exterior marks by drilling using NSK (Nakanishi Inc., Japan) variable speed drills and tungsten carbide drill bits with a "keyhole" methodology.

Bone was prepared using established protocols previously outlined (*49*–*51*). The method involves an ultrafiltration of the gelatinized bone collagen. Work at the ORAU suggests that the use of this technique for dating Paleolithic bone yields an improved reliability by more effective removal of low–molecular weight contaminants. Radiocarbon ages are given in table S1 as conventional ages B.P. (*52*), with B.P. representing radiocarbon years before present (1950 CE). We also provide our results in fM (fraction modern) space, which was used for calibration of the results. A bone-specific background correction was applied on the basis of multiple measurements of beyond ^{14}C age bone (*53*). This correction is used for all samples at the ORAU down to ~5 mg of collagen.

A suite of analytical methods was measured to assess the quality of the bone collagen extracts. These included C:N atomic ratios, % weight collagen, %C on combustion, %N, and stable isotopic values. The results are shown in table S2 for each bone sample that we dated. The samples we dated were acceptably well preserved in terms of collagen. Table S3 shows the output of the Bayesian model of all dates.

Luminescence dating

Principle and methods

Luminescence dating relies on the capacity of certain minerals to record the amount of natural radiation to which they have been exposed during burial. In the laboratory, the total amount of energy stored in the mineral is measured as a dose (Gy). The rate of energy absorption (dose rate, Gy/year) is derived from knowledge of the natural radioactivity in the sediment. The quotient of these two values (dose per dose rate) gives the burial time.

In this study, we have used two luminescence dating methods to provide age constraint on different types of mineral samples preserved

at Mandrin: optical dating [or optically stimulated luminescence (OSL) dating] and thermoluminescence (TL) dating. Optical dating is the method of determining the time elapsed since the last exposure of minerals to sunlight during transport and deposition. Generally, the preferred choice of mineral is quartz because of its common occurrence and its reliability as a natural dosimeter during the last ~150 ka (*54*). Quartz optical dating has been performed at two separate research laboratories (University of Oxford, UK, and University of Adelaide, Australia), each using different scales of equivalent dose (D_e) determination, with the aim of independently cross-checking the consistency of the resultant OSL chronologies.

TL dating allows determination of the time elapsed since flint artifacts were heated at elevated temperature (~400°C). This method therefore provides a direct age for the use of fires in the production or alteration of lithic artifacts. TL dating of burnt flint pieces was conducted at a third independent luminescence dating laboratory: Université Paris-Saclay, Gif-sur-Yvette, France. Full details of the multiple-grain OSL, single-grain OSL, and TL dating methods used in this study are provided in the Supplementary Materials and Methods.

Bayesian age modeling

The majority of the produced radiocarbon determinations, as well as the suite of OSL and TL ages, were used to construct a Bayesian model. The model consists of a sequence of individual radiocarbon and luminescence dates grouped within phases and ordered sequentially by depth (see Fig. 8). We used OxCal 4.4 software (*55*) and the INTCAL20 calibration curve (*56*). Bayesian modeling enables the relative stratigraphic information gleaned from the site during the excavation to be incorporated formally along with the calibrated likelihoods. The updated INTCAL20 curve extends back to 55,000 cal. B.P. and ensures that dates up to about this age can be calibrated reliably. We included radiocarbon dates from the post–Neronian II layers, B2 and C. In contrast to previous results (e.g., Ly-2755 from level 6, which gave a result of 33,300 ± 230 B.P.), all of the determinations from layer E and layers below it in the site produced greater than ages, indicating that their age was approaching or beyond our measurable limit of 49,900 B.P. (0.002 fM). The radiocarbon determinations from archeological levels below layer D were characterized by "greater than" ages, which suggest that the true age lies beyond the radiocarbon limit. This means that it is very difficult to calibrate them. For this reason, we applied minimum age constraints within the models in layers E and D, as outlined in the chronological query language (CQL) code for the model shown below. We used a general *t* outlier model (*57*) to quantify the divergence of certain likelihoods from the prior framework in the model. Some determinations were given higher outlier probabilities because of uncertainties in terms of context and location; these are listed in table S1. Most were given probabilities of 0.05; those with higher uncertainties were given 0.25 probability. The posterior outlier results suggested results around the same as the prior assigned probability, while the same was the case of those assigned higher uncertainties. The values are shown along with the Bayesian model in Fig. 8. Convergence for the model was high, averaging 99%, suggesting that the Markov chain Monte Carlo found solutions rapidly and, therefore, that the model is robust. The Bayesian model CQL code can be found in the Supplementary Materials and Methods.

The Mandrin model and the age estimate for the layer E Neronian substantially predate the start boundaries for the Uluzzian and Châtelperronian as previously published. When compared against the range for the final Mousterian (*16*), it is clearly earlier as well. It also ranges substantially earlier than determinations obtained from the Peştera-cu-Oase (*58*), Fumane, Bombrini, and Cavallo modern human and Protoaurignacian sites (*10*, *11*). While Ksar Akil is a fundamental archeological sequence for any questions on the beginnings of the Upper Paleolithic in western Eurasia, in terms of chronology, the case of Ksar Akil is controversial and cannot be resolved easily at present without more work and perhaps even new fieldwork and excavation. Recent dating studies of the site have produced divergent results, and its chronology remains an ongoing discussion (*30*, *59*, *60*). The reasons for these divergences are themselves part of the controversy. The sequence itself is relatively complex with excavations undertaken in different periods, first in 1937–1938 and a second phase 10 years later. The archeological collections are also located in several institutions, including the British Museum, the Peabody Museum in Cambridge (MA), and the Naturalis Biodiversity Center in Leiden. Because of the divergent radiometric results, no definitive ages or firm chronological conclusions can currently be proposed for the IUP and EUP parts of this key sequence. To provide a probability distribution function for the IUP in the Levant, we have instead focused on the best available remaining chronological evidence for this region, which at present is arguably the Boker Tachtit sequence. This sequence is well excavated and has a small number of well-provenanced and reliably dated samples analyzed in the Groningen facility. This forms the basis for our western Asian IUP start date comparison, which shows, in fig. S20, that Mandrin E is earlier than the Boker IUP (*61*). Future work, both at Ksar Akil and other Levantine sites, will hopefully improve the chronometric resolution we have for the important IUP industries in the Levant. Last, the Neronian age also predates the ages published for 11 heated flint samples from the IUP of Brno-Bohunice (*62*) in Central Europe (fig. S20). This suggests that the Neronian may be the earliest manifestation we have for this type of industry in Eurasia or that more chronometric work using the latest techniques is required from more sites so that we can be sure of the age relationship between the various facies.

While we cannot rule out the possibility that the IUP settlement of Mandrin E may be older than the Levantine ones, we caution here on premature conclusions. Obtaining precise chronologies for sites older than 50 ka is particularly challenging, and it is likely that this is the very high resolution obtained in Grotte Mandrin after 30 years of continuous efforts that makes it artificially appear chronologically older than the Levantine counterparts. Recent revisions of the Boker Tachtit site revealed that the IUP started earlier than previously recognized in the Levant, likely before 50 ka (*63*). While the chronology of Ksar Akil IUP remains debated [very possibly older than 46 ka (*30*, *59*, *60*)], the respective chronological position of Boker Tachtit and Mandrin level E is of great interest, even if we cannot rule out the possibility that the Neronian of Mandrin E is slightly older than the oldest IUP found in the Levant.

Molecular analyses

DNA extraction and sequencing

Before deciding whether ancient DNA extraction of rare, precious hominin remains could be successful, we assessed the overall DNA preservation rate at Mandrin using six equid teeth excavated from layers B to G. They were processed in the ancient DNA facilities of the CAGT laboratory, University Paul Sabatier, Toulouse, France, following the standard procedures described in (*64*). The surface of each sample was abraded using a drill, and a total of 40 to 70 mg of tooth root was cut off and powdered manually using a mortar.

The tooth powder was then extracted for ancient DNA following "method Y" of (*65*), with slight modifications. This method consists of a first digestion within 1 ml of extraction buffer [0.45 M EDTA, proteinase K (0.25 mg/ml), and 0.05% Tween 20], carried out for 1 hour at 37°C. After centrifugation for 2 min at 16,000*g*, the supernatant (referred to as E1) was recovered for further purification, while the remaining pellets were fully digested following an overnight digestion at 42°C within 1 ml of fresh extraction buffer. The corresponding digestion was recovered after centrifugation for 2 min at 13,000 rpm, referred to as supernatant E2. Both E1 and E2 were purified using MinElute columns (Qiagen), where the DNA elution consisted of two steps: first, 23 µl of elution buffer (Qiagen EB + 0.05% Tween 20) was incubated on the column for 10 min at 37°C and recovered following 1-min centrifugation at 6000 rpm. Second, the eluate was placed again on the column for a 10-min incubation at 37°C and centrifuged for 2 min at 13,000 rpm. This provided the final DNA extracts.

Each DNA extract was subjected to Uracil-Specific Excision Reagent treatment by incubation at 37°C for 3 hours with 7 µl of USER enzyme (NEB) to limit the impact of nucleotide misincorporations in downstream analysis. Illumina sequencing libraries were built following a protocol first described in (*66*) and adapted in (*64*), introducing a unique barcode of 7 nucleotides (nt) within adapter P5 and within adapter P7 before their adapter ligation. Libraries were enriched and indexed by performing 12 polymerase chain reaction (PCR) cycles in 25 µl of reactions using 1 U of AccuPrimeTM Pfx DNA polymerase, 3 µl of DNA library, and with an overall concentration of 0.2 µM of each primer, including the InPE1.0 primer and one custom PCR primer. The latter includes a 6-nt sequence tag index used for sequence demultiplexing. After purification using AMPure XP beads (1.4:1 beads:DNA ratio) and elution in 20 µl of EB + 0.05% Tween 20, library concentration and size were checked on a TapeStation 2200 instrument (Agilent technologies). Final libraries were pooled with other indexed libraries and Paired-end sequenced (80–base pair read length) on a MiniSeq instrument (Illumina).

Read processing and mapping

Illumina reads were processed and aligned against the horse mitochondrial reference sequence (GenBank accession no. NC_001640) (*67*) and the horse nuclear reference sequence [EquCab2; (*68*)] using the PALEOMIX version 1.1.1 pipeline (*69*) with default parameters, except that seeding was disabled. Illumina sequencing reads were trimmed for adapter sequences using AdapterRemoval2 (*70*). When overlapping for at least 11 nt and with a maximal edit distance of 1, paired-end reads were collapsed and further treated as single-end reads. Read mapping was carried out with BWA version 0.7.17-r1194-dirty, disabling seed, disregarding alignments showing mapping qualities inferior to 25. Summary statistics, including the total number of read pairs generated and endogenous DNA content per library (especially the fraction of high-quality hits mapping uniquely against the reference genomes considered), were directly obtained from PALEOMIX (table S12).

SUPPLEMENTARY MATERIALS

Supplementary material for this article is available at https://science.org/doi/10.1126/sciadv.abj9496

REFERENCES AND NOTES

1. J.-J. Hublin, A. Ben-Ncer, S. E. Bailey, S. E. Freidline, S. Neubauer, M. M. Skinner, I. Bergmann, A. le Cabec, S. Benazzi, K. Harvati, P. Gunz, New fossils from Jebel Irhoud, Morocco and the pan-African origin of *Homo sapiens*. *Nature* **546**, 289–292 (2017).
2. E. M. L. Scerri, M. G. Thomas, A. Manica, P. Gunz, J. T. Stock, C. Stringer, M. Grove, H. S. Groucutt, A. Timmermann, G. P. Rightmire, F. d'Errico, C. A. Tryon, N. A. Drake, A. S. Brooks, R. W. Dennell, R. Durbin, B. M. Henn, J. Lee-Thorp, P. deMenocal, M. D. Petraglia, J. C. Thompson, A. Scally, L. Chikhi, Did our species evolve in subdivided populations across Africa, and why does it matter? *Trends Ecol. Evol.* **33**, 582–594 (2018).
3. C. Stringer, The origin and evolution of *Homo sapiens*. *Philos. Trans. R. Soc. B* **371**, 20150237 (2016).
4. K. Harvati, C. Röding, A. M. Bosman, F. A. Karakostis, R. Grün, C. Stringer, P. Karkanas, N. C. Thompson, V. Koutoulidis, L. A. Moulopoulos, V. G. Gorgoulis, M. Kouloukoussa, Apidima Cave fossils provide earliest evidence of *Homo sapiens* in Eurasia. *Nature* **571**, 500–504 (2019).
5. J.-J. Hublin, The modern human colonization of western Eurasia: When and where? *Quat. Sci. Rev.* **118**, 194–210 (2015).
6. I. Hershkovitz, O. Marder, A. Ayalon, M. Bar-Matthews, G. Yasur, E. Boaretto, V. Caracuta, B. Alex, A. Frumkin, M. Goder-Goldberger, P. Gunz, R. L. Holloway, B. Latimer, R. Lavi, A. Matthews, V. Slon, D. B. Y. Mayer, F. Berna, G. Bar-Oz, R. Yeshurun, H. May, M. G. Hans, G. W. Weber, O. Barzilai, Levantine cranium from Manot Cave (Israel) foreshadows the first European modern humans. *Nature* **520**, 216–219 (2015).
7. W. Liu, M. Martinón-Torres, Y. J. Cai, S. Xing, H. W. Tong, S. W. Pei, M. J. Sier, X. H. Wu, R. L. Edwards, H. Cheng, Y. Y. Li, X. X. Yang, J. M. B. de Castro, X. J. Wu, The earliest unequivocally modern humans in southern China. *Nature* **526**, 696–699 (2015).
8. C. Clarkson, Z. Jacobs, B. Marwick, R. Fullagar, L. Wallis, M. Smith, R. G. Roberts, E. Hayes, K. Lowe, X. Carah, S. A. Florin, J. McNeil, D. Cox, L. J. Arnold, Q. Hua, J. Huntley, H. E. A. Brand, T. Manne, A. Fairbairn, J. Shulmeister, L. Lyle, M. Salinas, M. Page, K. Connell, G. Park, K. Norman, T. Murphy, C. Pardoe, Human occupation of northern Australia by 65,000 years ago. *Nature* **547**, 306–310 (2017).
9. A. Moroni, A. Ronchitelli, S. Arrighi, D. Aureli, S. Bailey, P. Boscato, F. Boschin, G. Capecchi, J. Crezzini, K. Douka, G. Marciani, D. Panetta, F. Ranaldo, S. Ricci, S. Scaramucci, V. Spagnolo, S. Benazzi, P. Gambassini, Grotta del Cavallo (Apulia – Southern Italy). The Uluzzian in the mirror. *J. Anthropol. Sci.* **96**, 125–160 (2018).
10. S. Benazzi, V. Slon, S. Talamo, F. Negrino, M. Peresani, S. E. Bailey, S. Sawyer, D. Panetta, G. Vicino, E. Starnini, M. A. Mannino, P. A. Salvadori, M. Meyer, S. Paabo, J. J. Hublin, The makers of the Protoaurignacian and implications for Neandertal extinction. *Science* **348**, 793–796 (2015).
11. S. Benazzi, K. Douka, C. Fornai, C. C. Bauer, O. Kullmer, J. Svoboda, I. Pap, F. Mallegni, P. Bayle, M. Coquerelle, S. Condemi, A. Ronchitelli, K. Harvati, G. W. Weber, Early dispersal of modern humans in Europe and implications for Neanderthal behaviour. *Nature* **479**, 525–528 (2011).
12. M. Peresani, S. Bertola, D. Delpiano, S. Benazzi, M. Romandini, The Uluzzian in the north of Italy: Insights around the new evidence at Riparo Broion. *Archaeol. Anthropol. Sci.* **11**, 3503–3536 (2019).
13. J.-J. Hublin, N. Sirakov, V. Aldeias, S. Bailey, E. Bard, V. Delvigne, E. Endarova, Y. Fagault, H. Fewlass, M. Hajdinjak, B. Kromer, I. Krumov, J. Marreiros, N. L. Martisius, L. Paskulin, V. Sinet-Mathiot, M. Meyer, S. Pääbo, V. Popov, Z. Rezek, S. Sirakova, M. M. Skinner, G. M. Smith, R. Spasov, S. Talamo, T. Tuna, L. Wacker, F. Welker, A. Wilcke, N. Zahariev, S. P. McPherron, T. Tsanova, Initial Upper Palaeolithic *Homo sapiens* from Bacho Kiro Cave, Bulgaria. *Nature* **581**, 299–302 (2020).
14. P. Semal, H. Rougier, I. Crevecoeur, C. Jungels, D. Flas, A. Hauzeur, B. Maureille, M. Germonpré, H. Bocherens, S. Pirson, L. Cammaert, N. de Clerck, A. Hambucken, T. Higham, M. Toussaint, J. van der Plicht, New data on the late Neandertals: Direct dating of the Belgian Spy fossils. *Am. J. Phys. Anthropol.* **138**, 421–428 (2009).
15. J.-J. Hublin, S. Talamo, M. Julien, F. David, N. Connet, P. Bodu, B. Vandermeersch, M. P. Richards, Radiocarbon dates from the Grotte du Renne and Saint-Césaire support a Neandertal origin for the Châtelperronian. *Proc. Natl. Acad. Sci. U.S.A.* **109**, 18743–18748 (2012).
16. T. Higham, K. Douka, R. Wood, C. B. Ramsey, F. Brock, L. Basell, M. Camps, A. Arrizabalaga, J. Baena, C. Barroso-Ruíz, C. Bergman, C. Boitard, P. Boscato, M. Caparrós, N. J. Conard, C. Draily, A. Froment, B. Galván, P. Gambassini, A. Garcia-Moreno, S. Grimaldi, P. Haesaerts, B. Holt, M. J. Iriarte-Chiapusso, A. Jelinek, J. F. Jordá Pardo, J. M. Maíllo-Fernández, A. Marom, J. Maroto, M. Menéndez, L. Metz, E. Morin, A. Moroni, F. Negrino, E. Panagopoulou, M. Peresani, S. Pirson, M. de la Rasilla, J. Riel-Salvatore, A. Ronchitelli, D. Santamaria, P. Semal, L. Slimak, J. Soler, N. Soler, A. Villaluenga, R. Pinhasi, R. Jacobi, The timing and spatiotemporal patterning of Neanderthal disappearance. *Nature* **512**, 306–309 (2014).
17. F. Welker, M. Hajdinjak, S. Talamo, K. Jaouen, M. Dannemann, F. David, M. Julien, M. Meyer, J. Kelso, I. Barnes, S. Brace, P. Kamminga, R. Fischer, B. M. Kessler, J. R. Stewart, S. Pääbo, M. J. Collins, J. J. Hublin, Palaeoproteomic evidence identifies archaic hominins associated with the Châtelperronian at the Grotte du Renne. *Proc. Natl. Acad. Sci. U.S.A.* **113**, 11162–11167 (2016).
18. D. Richter, G. Tostevin, P. Škrdla, W. Davies, New radiometric ages for the early Upper Palaeolithic type locality of Brno-Bohunice (Czech Republic): Comparison of OSL, IRSL, TL and ^{14}C dating results. *J. Archaeol. Sci.* **36**, 708–720 (2009).

19. B. Gravina, F. Bachellerie, S. Caux, E. Discamps, J.-P. Faivre, A. Galland, A. Michel, N. Teyssandier, J.-G. Bordes, No reliable evidence for a Neanderthal-Châtelperronian association at La Roche-à-Pierrot, Saint-Césaire. *Sci. Rep.* **8**, 15134 (2018).
20. L. Slimak, For a cultural anthropology of the last Neanderthals. *Quat. Sci. Rev.* **217**, 330–339 (2019).
21. M. Cortés-Sánchez, F. J. Jiménez-Espejo, M. D. Simón-Vallejo, C. Stringer, M. C. Lozano Francisco, A. García-Alix, J. L. Vera Peláez, C. P. Odriozola, J. A. Riquelme-Cantal, R. Parrilla Giráldez, A. Maestro González, N. Ohkouchi, A. Morales-Muñiz, An early Aurignacian arrival in southwestern Europe. *Nat. Ecol. Evol.* **3**, 207–212 (2019).
22. L. Slimak, Sociodiversity and paradoxes from the end of the Middle Paleolithic to the emergence of the Upper Paleolithic, in *The Third Man. The Prehistory of the Altaï*, J. J. Cleyet–Merle, M. V. Shunkov, J. M. Geneste, A. P. Derevianko, L. Slimak, A. L. Krivoshapkin, B. Gravina, A. Turq, B. Maureille, Eds. (Éditions de la Réunion des musées nationaux – Grand Palais, 2017), pp. 125–133.
23. V. P. Chabai, A. Marks, K. Monigal, Crimea in the context of the Eastern European Middle Paleolithic and Early Upper Paleolithic, in *The Middle Paleolithic and Early Upper Paleolithic of Eastern Crimea*, V. P. Chabai, K. Monigal, A. E. Marks, Eds. (ERAUL, Liège, 2004), pp. 419–460.
24. P. R. Nigst, P. Haesaerts, F. Damblon, C. Frank-Fellner, C. Mallol, B. Viola, M. Götzinger, L. Niven, G. Trnka, J. J. Hublin, Early modern human settlement of Europe north of the Alps occurred 43,500 years ago in a cold steppe-type environment. *Proc. Natl. Acad. Sci. U.S.A.* **111**, 14394–14399 (2014).
25. L. Slimak, The Neronian and the historical structure of cultural shifts from Middle to Upper Palaeolithic in Mediterranean France. *J. Archaeol. Sci.* **35**, 2204–2214 (2008).
26. J. Combier, *Le Paléolithique de l'Ardèche dans son Cadre Paléoclimatique*. Mémoire de l'Institute de Préhistoire de l'Université de Bordeaux 4 (Delmas, 1967).
27. L. Metz, *Néandertal en armes? Des armes, et de l'arc, au tournant du 50ème millénaire en France Méditerranéenne*, thesis, Aix-Marseille University, France (2015).
28. J. Combier, De la fin du Moustérien au Paléolithique supérieur. Les données de la région rhodanienne, in *Paléolithique moyen récent et Paléolithique supérieur ancien. Ruptures et transitions : Examen critique de documents archéologiques*, C. Farizy, Ed. (Musée de Préhistoire d'Île de France, 1990), pp. 267–277.
29. L. Slimak, Sur un point de vue heuristique concernant la production et la transformation de support au Paléolithique moyen. *Gallia Préhistoire* **50**, 1–22 (2008).
30. M. D. Bosch, M. A. Mannino, A. L. Prendergast, T. C. O'Connell, B. Demarchi, S. M. Taylor, L. Niven, J. van der Plicht, J. J. Hublin, New chronology for Ksâr 'Akil (Lebanon) supports Levantine route of modern human dispersal into Europe. *Proc. Natl. Acad. Sci. U.S.A.* **112**, 7683–7688 (2015).
31. K. Douka, C. A. Bergman, R. E. M. Hedges, F. P. Wesselingh, T. F. G. Higham, Chronology of Ksar Akil (Lebanon) and implications for the colonization of Europe by anatomically modern humans. *PLOS ONE* **8**, e72931 (2013).
32. P. Skrdla, Comparison of Boker Tachtit and Stranska Skala MP/UP transitional industries. *J. Israel Prehistoric Soc.* **33**, 37–73 (2003).
33. I. Azoury, *Ksar Akil, Lebanon: A Technological and Typological Analysis of the Transitional and Early Upper Palaeolithic Levels of Ksar Akil and Abu Halka. Vol. I, Levels XXV-XII* (BAR International Series, 1986).
34. C. A. Bergman, Synthèse Paléolithique supérieur. *Paléorient* **14**, 223–227 (1988).
35. S. L. Kuhn, M. C. Stiner, D. S. Reese, E. Güleç, Ornaments of the earliest Upper Paleolithic: New insights from the Levant. *Proc. Natl. Acad. Sci. U.S.A.* **98**, 7641–7646 (2001).
36. K. Ohnuma, C. A. Bergman, A Technological Analysis of the Upper Paleolithic Levels (XXV-VI) of Ksar Akil, Lebanon, in *The Emergence of Modern Humans: An Archaeological Perspective*, P. Mellars, (Edinburgh Univ. Press, 1990), pp. 91–138.
37. C. A. Bergman, C. B. Stringer, Fifty years after: Egbert, an Early Upper Palaeolithic juvenile from Ksar Akil, Lebanon. *Paléorient* **15**, 99–111 (1989).
38. M. Kuhlwilm, I. Gronau, M. J. Hubisz, C. de Filippo, J. Prado-Martinez, M. Kircher, Q. Fu, H. A. Burbano, C. Lalueza-Fox, M. de la Rasilla, A. Rosas, P. Rudan, D. Brajkovic, Ž. Kucan, I. Gušic, T. Marques-Bonet, A. M. Andrés, B. Viola, S. Pääbo, M. Meyer, A. Siepel, S. Castellano, Ancient gene flow from early modern humans into Eastern Neanderthals. *Nature* **530**, 429–433 (2016).
39. F. A. Villanea, J. G. Schraiber, Multiple episodes of interbreeding between Neanderthal and modern humans. *Nat. Ecol. Evol.* **3**, 39–44 (2019).
40. M. J. Hubisz, A. L. Williams, A. Siepel, Mapping gene flow between ancient hominins through demography-aware inference of the ancestral recombination graph. *bioRxiv*, 687368 (2019).
41. B. Vernot, S. Tucci, J. Kelso, J. G. Schraiber, A. B. Wolf, R. M. Gittelman, M. Dannemann, S. Grote, R. C. McCoy, H. Norton, L. B. Scheinfeldt, D. A. Merriwether, G. Koki, J. S. Friedlaender, J. Wakefield, S. Pääbo, J. M. Akey, Excavating Neandertal and Denisovan DNA from the genomes of Melanesian individuals. *Science* **352**, 235–239 (2016).
42. A. B. Wolf, J. M. Akey, Outstanding questions in the study of archaic hominin admixture. *PLOS Genet.* **14**, e1007349 (2018).
43. J. D. Wall, M. A. Yang, F. Jay, S. K. Kim, E. Y. Durand, L. S. Stevison, C. Gignoux, A. Woerner, M. F. Hammer, M. Slatkin, Higher levels of neanderthal ancestry in East Asians than in Europeans. *Genetics* **194**, 199–209 (2013).
44. S. Sankararaman, N. Patterson, H. Li, S. Pääbo, D. Reich, The date of interbreeding between neandertals and modern humans. *PLOS Genet.* **8**, e1002947 (2012).
45. Q. Fu, M. Hajdinjak, O. T. Moldovan, S. Constantin, S. Mallick, P. Skoglund, N. Patterson, N. Rohland, I. Lazaridis, B. Nickel, B. Viola, K. Prüfer, M. Meyer, J. Kelso, D. Reich, S. Pääbo, An early modern human from Romania with a recent Neanderthal ancestor. *Nature* **524**, 216–219 (2015).
46. M. Hajdinjak, Q. Fu, A. Hübner, M. Petr, F. Mafessoni, S. Grote, P. Skoglund, V. Narasimham, H. Rougier, I. Crevecoeur, P. Semal, M. Soressi, S. Talamo, J. J. Hublin, I. Gušić, Ž. Kućan, P. Rudan, L. V. Golovanova, V. B. Doronichev, C. Posth, J. Krause, P. Korlević, S. Nagel, B. Nickel, M. Slatkin, N. Patterson, D. Reich, K. Prüfer, M. Meyer, S. Pääbo, J. Kelso, Reconstructing the genetic history of late Neanderthals. *Nature* **555**, 652–656 (2018).
47. S. Vandevelde, J. É. Brochier, C. Petit, L. Slimak, Establishment of occupation chronicles in Grotte Mandrin using sooted concretions: Rethinking the Middle to Upper Paleolithic transition. *J. Hum. Evol.* **112**, 70–78 (2017).
48. S. Vandevelde, *Y'a pas de suie sans feu ! Étude micro-chronologique des concrétions fuligineuses. Étude de cas : Le site paléolithique de la Grotte Mandrin (France) [There's no soot without fire! Micro-chronological study of fuliginous speleothems. Case study: The Grotte of Mandrin (France) Paleolithic site]*, thesis, Université de Paris 1 – Panthéon-Sorbonne (2019).
49. T. F. G. Higham, R. M. Jacobi, C. Bronk Ramsey, AMS radiocarbon dating of ancient bone using ultrafiltration. *Radiocarbon* **48**, 179–195 (2006).
50. C. Bronk Ramsey, T. F. G. Higham, A. Bowles, R. Hedges, Improvements to the pretreatment of bone at Oxford. *Radiocarbon* **46**, 155–163 (2004).
51. F. Brock, C. Bronk Ramsey, T. F. G. Higham, Quality Assurance of ultrafiltered bone dating. *Radiocarbon* **49**, 187–192 (2007).
52. M. Stuiver, H. A. Polach, Discussion reporting of ^{14}C data. *Radiocarbon* **19**, 355–363 (1977).
53. R. E. Wood, C. Bronk Ramsey, T. F. G. Higham, Refining the ultrafiltration bone pretreatment background for radiocarbon dating at ORAU. *Radiocarbon* **52**, 600–611 (2010).
54. A. G. Wintle, A. S. Murray, A review of quartz optically stimulated luminescence characteristics and their relevance in single-aliquot regeneration dating protocols. *Radiat. Meas.* **41**, 369–391 (2006).
55. C. Bronk Ramsey, Bayesian analysis of radiocarbon dates. *Radiocarbon* **51**, 337–360 (2009).
56. P. J. Reimer, W. E. N. Austin, E. Bard, A. Bayliss, P. G. Blackwell, C. B. Ramsey, M. Butzin, H. Cheng, R. L. Edwards, M. Friedrich, P. M. Grootes, T. P. Guilderson, I. Hajdas, T. J. Heaton, A. G. Hogg, K. A. Hughen, B. Kromer, S. W. Manning, R. Muscheler, J. G. Palmer, C. Pearson, J. van der Plicht, R. W. Reimer, D. A. Richards, E. M. Scott, J. R. Southon, C. S. M. Turney, L. Wacker, F. Adolphi, U. Büntgen, M. Capano, S. M. Fahrni, A. Fogtmann-Schulz, R. Friedrich, P. Köhler, S. Kudsk, F. Miyake, J. Olsen, F. Reinig, M. Sakamoto, A. Sookdeo, S. Talamo, The IntCal20 Northern Hemisphere radiocarbon age calibration curve (0–55 cal kBP). *Radiocarbon* **62**, 725–757 (2020).
57. C. Bronk Ramsey, Dealing with outliers and offsets in radiocarbon dating. *Radiocarbon* **51**, 1023–1045 (2009).
58. E. Trinkaus, O. Moldovan, Milota, A. Bilgar, L. Sarcina, S. Athreya, S. E. Bailey, R. Rodrigo, G. Mircea, T. Higham, C. B. Ramsey, J. van der Plicht, An Early Modern Human from the Peştera cu Oase, Romania. *Proc. Natl. Acad. Sci. U.S.A.* **100**, 11231–11236 (2003).
59. K. Douka, T. F. G. Higham, C. Bergman, Statistical and archaeological errors invalidate the proposed chronology for the site of Ksar Akil. *Proc. Natl. Acad. Sci. U.S.A.* **112**, E7034 (2015).
60. M. Bosch, M. A. Mannino, A. L. Prendergast, T. C. O'Connell, B. Demarchi, S. M. Taylor, L. Niven, J. van der Plicht, J.-J. Hublin, Reply to Douka *et al.*: Critical evaluation of the Ksâr 'Akil chronologies. *Proc. Natl. Acad. Sci. U.S.A.* **112**, E7035 (2015).
61. S. L. Kuhn, N. Zwyns, Rethinking the initial Upper Paleolithic. *Quat. Int.* **347**, 29–38 (2014).
62. D. Richter, G. Tostevin, P. Škrdla, Bohunician technology and thermoluminescence dating of the type locality of Brno-Bohunice (Czech Republic). *J. Hum. Evol.* **55**, 871–885 (2008).
63. E. Boaretto, M. Hernandez, M. Goder-Goldberger, V. Aldeias, L. Regev, V. Caracuta, S. P. McPherron, J. J. Hublin, S. Weiner, O. Barzilai, The absolute chronology of Boker Tachtit (Israel) and implications for the Middle to Upper Paleolithic transition in the Levant. *Proc. Natl. Acad. Sci. U.S.A.* **118**, e2014657118 (2021).
64. C. Gaunitz, A. Fages, K. Hanghøj, A. Albrechtsen, N. Khan, M. Schubert, A. Seguin-Orlando, I. J. Owens, S. Felkel, O. Bignon-Lau, P. de Barros Damgaard, A. Mittnik, A. F. Mohaseb, H. Davoudi, S. Alquraishi, A. H. Alfarhan, K. A. S. al-Rasheid, E. Crubézy, N. Benecke, S. Olsen, D. Brown, D. Anthony, K. Massy, V. Pitulko, A. Kasparov, G. Brem, M. Hofreiter, G. Mukhtarova, N. Baimukhanov, L. Lõugas, V. Onar, P. W. Stockhammer, J. Krause, B. Boldgiv, S. Undrakhbold, D. Erdenebaatar, S. Lepetz, M. Mashkour, A. Ludwig,

B. Wallner, V. Merz, I. Merz, V. Zaibert, E. Willerslev, P. Librado, A. K. Outram, L. Orlando, Ancient genomes revisit the ancestry of domestic and Przewalski's horses. *Science* **360**, 111–114 (2018).
65. C. Gamba, K. Hanghøj, C. Gaunitz, A. H. Alfarhan, S. A. Alquraishi, K. A. S. al-Rasheid, D. A. N. I. E. L. G. Bradley, L. Orlando, Comparing the performance of three ancient DNA extraction methods for high-throughput sequencing. *Mol. Ecol. Resour.* **16**, 459–469 (2016).
66. N. Rohland, E. Harney, S. Mallick, S. Nordenfelt, D. Reich, Partial uracil-DNA-glycosylase treatment for screening of ancient DNA. *Philos. Trans. R. Soc. Lond. Ser. B Biol. Sci.* **370**, 20130624 (2015).
67. X. Xiufeng, U. Árnason, The complete mitochondrial DNA sequence of the horse, *Equus caballus*: Extensive heteroplasmy of the control region. *Gene* **148**, 357–362 (1994).
68. C. M. Wade, E. Giulotto, S. Sigurdsson, M. Zoli, S. Gnerre, F. Imsland, T. L. Lear, D. L. Adelson, E. Bailey, R. R. Bellone, H. Blöcker, O. Distl, R. C. Edgar, M. Garber, T. Leeb, E. Mauceli, J. N. MacLeod, M. C. T. Penedo, J. M. Raison, T. Sharpe, J. Vogel, L. Andersson, D. F. Antczak, T. Biagi, M. M. Binns, B. P. Chowdhary, S. J. Coleman, G. Della Valle, S. Fryc, G. Guérin, T. Hasegawa, E. W. Hill, J. Jurka, A. Kiialainen, G. Lindgren, J. Liu, E. Magnani, J. R. Mickelson, J. Murray, S. G. Nergadze, R. Onofrio, S. Pedroni, M. F. Piras, T. Raudsepp, M. Rocchi, K. H. Røed, O. A. Ryder, S. Searle, L. Skow, J. E. Swinburne, A. C. Syvänen, T. Tozaki, S. J. Valberg, M. Vaudin, J. R. White, M. C. Zody; Broad Institute Genome Sequencing Platform; Broad Institute Whole Genome Assembly Team, E. S. Lander, K. Lindblad-Toh, Genome sequence, comparative analysis, and population genetics of the domestic horse. *Science* **326**, 865–867 (2009).
69. M. Schubert, L. Ermin, C. D. Sarkissian, H. Jónsson, A. Ginolhac, R. Schaefer, M. D. Martin, R. Fernández, M. Kircher, M. McCue, E. Willerslev, L. Orlando, Characterization of ancient and modern genomes by SNP detection and phylogenomic and metagenomic analysis using PALEOMIX. *Nat. Protoc.* **9**, 1056–1082 (2014).
70. M. Schubert, S. Lindgreen, L. Orlando, AdapterRemoval v2: Rapid adapter trimming, identification, and read merging. *BMC. Res. Notes* **9**, 88 (2016).
71. C. F. Spoor, F. W. Zonneveld, G. A. Macho, Linear measurements of cortical bone and dental enamel by computed tomography: Applications and problems. *Am. J. Phys. Anthropol.* **91**, 469–484 (1993).
72. R. J. Fajardo, T. M. Ryan, J. Kappelman, Assessing the accuracy of high-resolution X-ray computed tomography of primate trabecular bone by comparisons with histological sections. *Am. J. Phys. Anthropol.* **118**, 1–10 (2002).
73. M. N. Coleman, M. W. Colbert, Technical note: CT thresholding protocols for taking measurements on three-dimensional models. *Am. J. Phys. Anthropol.* **133**, 723–725 (2007).
74. S. Benazzi, S. E. Bailey, M. Peresani, M. A. Mannino, M. Romandini, M. P. Richards, J. J. Hublin, Middle Paleolithic and Uluzzian human remains from Fumane Cave, Italy. *J. Hum. Evol.* **70**, 61–68 (2014).
75. M. Toussaint, A. J. Olejniczak, S. el Zaatari, P. Cattelain, D. Flas, C. Letourneux, S. Pirson, The Neandertal lower right deciduous second molar from Trou de l'Abîme at Couvin, Belgium. *J. Hum. Evol.* **58**, 56–67 (2010).
76. J.-L. Voisin, S. Condemi, M. H. Wolpoff, D. W. Frayer, A new online database (http://anthropologicaldata.free.fr) and a short reflection about the productive use of compiling Internet data. *PaleoAnthropology* **2012**, 241–244 (2012).
77. B. Maureille, H. Rougier, F. Houët, B. Vandermeersch, Les dents inférieures du néandertalien Regourdou 1 (site de Regourdou, commune de Montignac, Dordogne): Analyses métriques et comparatives. *Paleo* **13**, 183–200 (2001).
78. H. Scolan, F. Santos, A.-M. Tillier, B. Maureille, A. Quintard, Des nouveaux vestiges néanderthaliens à Las Pélénos (Monsempron-Libos, Lot-et-Garonne, France). *Bull. Mém. Soc. Anthropol. Paris* **24**, 69–95 (2012).
79. R. Macchiarelli, P. Bayle, L. Bondioli, A. Mazurier, C. Zanolli, From outer to inner structural morphology in dental anthropology. The integration of the third dimension in the visualization and quantitative analysis of fossil remains, in *Anthropological Perspectives on Tooth Morphology: Genetics, Evolution, Variation*, R.G. Scott, J.D. Irish, Eds. (Cambridge Univ. Press; Cambridge, 2013), pp. 250–277.
80. C. Zanolli, P. Bayle, L. Bondiolin, M. C. Dean, M. L. Luyer, A. Mazurier, W. Morita, R. Macchiarelli, Is the deciduous/permanent molar enamel thickness ratio a taxon-specific indicator in extant and extinct hominids? *C.R. Palevol* **16**, 702–714 (2017).
81. C. Zanolli, M. Martinón-Torres, F. Bernardini, G. Boschian, A. Coppa, D. Dreossi, L. Mancini, M. Martínez de Pinillos, L. Martín-Francés, J. M. Bermúdez de Castro, C. Tozzi, C. Tuniz, R. Macchiarelli, The Middle Pleistocene (MIS 12) human dental remains from Fontana Ranuccio (Latium) and Visogliano (Friuli-Venezia Giulia), Italy. A comparative high resolution endostructural assessment. *PLOS ONE* **13**, e0189773 (2018).
82. K. Kupczik, L. K. Delezene, M. M. Skinner, Mandibular molar root and pulp cavity morphology in *Homo naledi* and other Plio-Pleistocene hominins. *J. Hum. Evol.* **130**, 83–95 (2019).
83. S. E. Bailey, S. Benazzi, J.-J. Hublin, Allometry, merism, and tooth shape of the upper deciduous m2 and permanent M1. *Am. J. Phys. Anthropol.* **154**, 104–114 (2014).
84. F.J. Rohlf, TpsDig2. *TpsSeries* (Department of Ecology and Evolution, SUNY, Stony Brook, New York, 2005).
85. S. E. Bailey, S. Benazzi, L. Buti, J.-J. Hublin, Allometry, merism, and tooth shape of the lower second deciduous molar and first permanent molar. *Am. J. Phys. Anthropol.* **159**, 93–105 (2016).
86. A. Cardini, P. D. Polly, Cross-validated between group PCA scatterplots: A solution to spurious group separation? *Evol. Biol.* **47**, 85–95 (2020).
87. P. Mitteroecker, F. L. Bookstein, Linear discrimination, ordination, and the visualization of selection gradients in modern morphometrics. *Evol. Biol.* **38**, 100–114 (2011).
88. A. Cardini, P. O'Higgins, F. J. Rohlf, Seeing distinct groups where there are none: Spurious patterns from between-group PCA. *Evol. Biol.* **46**, 303–316 (2019).
89. S. Schlager, Chapter 9 - Morpho and Rvcg – Shape Analysis in R: R-Packages for Geometric Morphometrics, Shape Analysis and Surface Manipulations, in *Statistical Shape and Deformation Analysis*, G. Zheng, S. Li, G. Szekely (London, Academic Press, 2017), pp. 217–256.
90. R Development Core Team. R: *A language and environment for statistical computing*.http://www.R-project.org. (2017).
91. F.L. Bookstein, *Morphometric Tools for Landmark Data: Geometry and Biology* (Cambridge Univ. Press, 1991).
92. G. Guerin, N. Mercier, G. Adamiec, Dose-rate conversion factors: Update. *Ancient TL* **29**, 5–8 (2011).
93. G. Guérin, N. Mercier, R. Nathan, G. Adamiec, Y. Lefrais, On the use of the infinite matrix assumption and associated concepts: A critical review. *Radiat. Meas.* **47**, 778–785 (2012).
94. N. Mercier, H. Valladas, G. Valladas, A new dosimetric calibration tool. *Nucl. Tracks Radiat. Meas.* **23**, 507–508 (1994).
95. V. J. Bortolot, A new modular high capacity OSL reader system. *Radiat. Meas.* **32**, 751–757 (2000).
96. J. R. Prescott, J. T. Hutton, Cosmic ray contributions to dose rates for luminescence and ESR dating: Large depths and long-term time variations. *Radiat. Meas.* **23**, 497–500 (1994).
97. F. De Corte, D. Vandenberghe, J. P. Buylaert, P. Van den Haute, J. Kucera, Relative and k0-standardized INAA to assess the internal (Th, U) radiation dose rate in the 'quartz coarse-grain protocol' for OSL dating of sediments: Unexpected observations. *Nucl. Instrum. Methods Phys. Res. A* **564**, 743–751 (2006).
98. D. Vandenberghe, F. De Corte, J. P. Buylaert, J. Kucera, P. Van den Haute, On the internal radioactivity in quartz. *Radiat. Meas.* **43**, 771–775 (2008).
99. D. Richter, A. Richter, K. Dornich, Lexsyg—A new system for luminescence research. *Geochronometria* **40**, 220–228 (2013).
100. D. Richter, R. Pintaske, K. Dornich, M. R. Krbetschek, A novel beta source design for uniform irradiation in dosimetric applications. *Ancient TL* **30**, 57–63 (2012).
101. A. S. Murray, A. G. Wintle, Luminescence dating of quartz using an improved single-aliquot regenerative-dose protocol. *Radiat. Meas.* **32**, 57–73 (2000).
102. G. A. T. Duller, Distinguishing quartz and feldspar in single grain luminescence measurements. *Radiat. Meas.* **37**, 161–165 (2003).
103. G. A. T. Duller, The Analyst software package for luminescence data: Overview and recent improvements. *Ancient TL* **33**, 35–42 (2015).
104. M. Dietze, S. Kreutzer, C. Burow, M. C. Fuchs, M. Fischer, C. Schmidt, The abanico plot: Visualizing chronometric data with individual standard errors. *Quat. Geochronol.* **9**, 54–64 (2012).
105. S. Kreutzer, C. Schmidt, M. C. Fuchs, M. Dietze, M. Fischer, M. Fuchs, Introducing an R package for luminescence dating analysis. *Ancient TL* **30**, 1–8 (2012).
106. L. J. Arnold, R. M. Bailey, G. E. Tucker, Statistical treatment of fluvial dose distributions from southern Colorado arroyo deposits. *Quat. Geochronol.* **2**, 162–167 (2007).
107. L. J. Arnold, R. G. Roberts, R. F. Galbraith, S. B. DeLong, A revised burial dose estimation procedure for optical dating of young and modern-age sediments. *Quat. Geochronol.* **4**, 306–325 (2009).
108. L. J. Arnold, M. Demuro, M. Navazo Ruiz, A. Benito-Calvo, A. Pérez-González, OSL dating of the Middle Palaeolithic Hotel California site, Sierra de Atapuerca, north-central Spain. *Boreas* **42**, 285–305 (2013).
109. L. J. Arnold, M. Demuro, N. A. Spooner, G. J. Prideaux, M. C. McDowell, A. B. Camens, E. H. Reed, J. M. Parés, J. L. Arsuaga, J. M. Bermúdez de Castro, E. Carbonell, Single-grain TT-OSL bleaching characteristics: Insights from modern analogues and OSL dating comparisons. *Quat. Geochronol.* **49**, 45–51 (2019).
110. M. Demuro, R. G. Roberts, D. G. Froese, L. J. Arnold, F. Brock, C. B. Ramsey, Optically stimulated luminescence dating of single and multiple grains of quartz from perennially frozen loess in western Yukon Territory, Canada: Comparison with radiocarbon chronologies for the late Pleistocene Dawson tephra. *Quat. Geochronol.* **3**, 346–364 (2008).
111. M. Demuro, L. J. Arnold, D. Froese, R. G. Roberts, OSL dating of loess deposits bracketing Sheep Creek tephra beds, northwest Canada: Dim and problematic single-grain OSL characteristics and their effect on multi-grain age estimates. *Quat. Geochronol.* **15**, 67–87 (2013).

112. M. J. Aitken, *An Introduction to Optical Dating: The Dating of Quaternary Sediments by the Use of Photon-stimulated Luminescence* (Oxford Univ. Press, 1998).
113. L. J. Arnold, M. Demuro, M. Navazo Ruiz, Empirical insights into multi-grain averaging effects from 'pseudo' single-grain OSL measurements. *Radiat. Meas.* **47**, 652–658 (2012).
114. L. Bøtter-Jensen, M. Mejdahl, Assessment of beta dose-rate using a GM multicounter system. *Nucl. Tracks Radiat. Meas.* **14**, 187–191 (1988).
115. P.J. Potts, M. Thompson, S.R.N. Chenery, P.C. Webb, H.U. Kasper, *Geopt13 - An International Proficiency Test for Analytical Geochemistry Laboratories - Report on Round 13 / July 2003 (Köln Loess)* (International Association of Geoanalysts, 2003).
116. B. J. Brennan, Beta doses to spherical grains. *Radiat. Meas.* **37**, 299–303 (2003).
117. O. Allkofer, *Introduction to Cosmic Radiation* (Verlag Karl Thiemig, Munich, 1974).
118. M. A. Smith, J. R. Prescott, M. J. Head, Comparison of ^{14}C and luminescence chronologies at Puritjarra Rock shelter, central Australia. *Quat. Sci. Rev.* **16**, 299–320 (1997).
119. V. Mejdahl, Internal radioactivity in quartz and feldspar grains. *Ancient TL* **5**, 10–17 (1987).
120. J. M. Bowler, H. Johnston, J. M. Olley, J. R. Prescott, R. G. Roberts, W. Shawcross, N. A. Spooner, New ages for human occupation and climatic change at Lake Mungo, Australia. *Nature* **421**, 837–840 (2003).
121. Z. Jacobs, G. A. T. Duller, A. G. Wintle, C. S. Henshilwood, Extending the chronology of deposits at Blombos Cave, South Africa, back to 140 ka using optical dating of single and multiple grains of quartz. *J. Hum. Evol.* **51**, 255–273 (2006).
122. S. M. Pawley, R. M. Bailey, J. Rose, B. S. P. Moorlock, R. J. O. Hamblin, S. J. Booth, J. R. Lee, Age limits on Middle Pleistocene glacial sediments from OSL dating, north Norfolk, UK. *Quat. Sci. Rev.* **27**, 1363–1377 (2008).
123. R. J. Lewis, J. Tibby, L. J. Arnold, C. Barr, J. Marshall, G. McGregor, P. Gadd, Y. Yokoyama, Insights into subtropical Australian aridity from Welsby Lagoon, North Stradbroke Island, over the past 80,000 years. *Quat. Sci. Rev.* **234**, 106262 (2020).
124. J. Rees-Jones, Optical dating of young sediments using fine-grain quartz. *Ancient TL* **13**, 9–14 (1995).
125. J. Rees-Jones, M. S. Tite, Optical dating results for British archaeological sediments. *Archaeometry* **39**, 177–187 (1997).
126. V. Mejdahl, Thermoluminescence dating: Beta-dose attenuation in quartz grains. *Archaeometry* **21**, 61–72 (1979).
127. M.J. Aitken, *Thermoluminescence Dating* (Academic Press, 1985).
128. M. L. Readhead, Thermoluminescence dose rate data and dating equations for the case of disequilibrium in the decay series. *Nucl. Tracks Radiat. Meas.* **13**, 197–207 (1987).
129. L. J. Arnold, M. Duval, C. Falguères, J.-J. Bahain, M. Demuro, Portable gamma spectrometry with cerium-doped lanthanum bromide scintillators: Suitability assessments for luminescence and electron spin resonance dating applications. *Radiat. Meas.* **47**, 6–18 (2012).
130. L. J. Arnold, M. Duval, M. Demuro, N. A. Spooner, M. Santonja, A. Pérez-González, OSL dating of individual quartz 'supergrains' from the Ancient Middle Palaeolithic site of Cuesta de la Bajada, Spain. *Quat. Geochronol.* **36**, 78–101 (2016).
131. R. F. Galbraith, A note on the variance of a background-corrected OSL count. *Ancient TL* **20**, 49–51 (2002).
132. G. A. T. Duller, Assessing the error on equivalent dose estimates derived from single aliquot regenerative dose measurements. *Ancient TL* **25**, 15–24 (2007).
133. V. Hansen, A. Murray, J.-P. Buylaert, E.-Y. Yeo, K. Thomsen, A new irradiated quartz for beta source calibration. *Radiat. Meas.* **81**, 123–127 (2015).
134. L. J. Arnold, R. G. Roberts, Stochastic modelling of multi-grain equivalent dose (D_e) distributions: Implications for OSL dating of sediment mixtures. *Quat. Geochronol.* **4**, 204–230 (2009).
135. R. M. Bailey, L. J. Arnold, Statistical modelling of single grain quartz De distributions and an assessment of procedures for estimating burial dose. *Quat. Sci. Rev.* **25**, 2475–2502 (2006).
136. L. J. Arnold, R. G. Roberts, Paper I – Optically Stimulated Luminescence (OSL) dating of perennially-frozen deposits in north-central Siberia: OSL characteristics of quartz grains and methodological considerations regarding their suitability for dating. *Boreas* **40**, 389–416 (2011).
137. R. F. Galbraith, R. G. Roberts, G. M. Laslett, H. Yoshida, J. M. Olley, Optical dating of single and multiple grains of quartz from Jinmium rock shelter, northern Australia: Part I, Experimental design and statistical models. *Archaeometry* **41**, 339–364 (1999).
138. L. J. Arnold, R. G. Roberts, R. D. E. MacPhee, E. Willerslev, A. N. Tikhonov, F. Brock, Optical dating of perennially frozen deposits associated with preserved ancient plant and animal DNA in north-central Siberia. *Quat. Geochronol.* **3**, 114–136 (2008).
139. L. J. Arnold, R. G. Roberts, R. D. E. Macphee, J. S. Haile, F. Brock, P. Möller, D. G. Froese, A. N. Tikhonov, A. R. Chivas, M. T. P. Gilbert, E. Willerslev, Paper II – Dirt, dates and DNA: OSL and radiocarbon chronologies of perennially frozen sediments in Siberia, and their implications for sedimentary ancient DNA studies. *Boreas* **40**, 417–445 (2011).
140. R. P. Nathan, P. J. Thomas, M. Jain, A. S. Murray, E. J. Rhodes, Environmental dose rate heterogeneity of beta radiation and its implications for luminescence dating: Monte Carlo modelling and experimental validation. *Radiat. Meas.* **37**, 305–313 (2003).
141. H. Valladas, Thermoluminescence dating of flint. *Quat. Sci. Rev.* **11**, 1–5 (1992).
142. G. Valladas, A gamma ray irradiator. *PACT* **3**, 439–442 (1978).
143. G. Guérin, J. C. Lefèvre, A low cost TL–OSL reader dedicated to high temperature studies. *Measurement* **49**, 26–33 (2014).
144. R. Sempéré, B. Charrière, F. Van Wambeke, G. Cauwet, Carbon inputs of the Rhône River to the Mediterranean Sea: Biogeochemical implications. *Glob. Biogeochem. Cycles* **14**, 669–681 (2000).
145. S. Vandevelde, J. É. Brochier, B. Desachy, C. Petit, L. Slimak, Sooted concretions: A new micro-chronological tool for high temporal resolution archaeology. *Quat. Int.* **474**, 103–118 (2018).
146. P. Goldberg, Micromorphology and site formation at Die Kelders Cave I, South Africa. *J. Hum. Evol.* **38**, 43–90 (2000).
147. G. Stoops, *Guidelines for Analysis and Description of Soil and Regolith Thin Sections* (Soil Science Society of America, Madison, WI, 2003).
148. V. Jacq, P. Albert, R. Delome, Le mistral – Quelques aspects des connaissances actuelles. *La Météorol.* **50**, 30–38 (2005).
149. L. K. Horowitz, P. Goldberg, A study of Pleistocene and Holocene hyaena coprolites. *J. Archaeol. Sci.* **16**, 71–94 (1989).
150. R. Macphail, P. Goldberg, Geoarchaeological Investigation of Sediments from Gorham's and Vanguard Caves, Gibraltar: Microstratigraphical (Soil Micromorphological and Chemical) Signatures, in *Neanderthals on the Edge* (eds Stringer, C., Barton, C.M. & Finlayson C.) 183–200 (Oxbow, 2000).
151. L. Slimak, Les Dernières Expressions du Moustérien entre Loire et Rhône. Phd thesis, Université de Provence (2004).
152. L. Slimak, Le Néronien et la structure historique du basculement du Paléolithique moyen au Paléolithique supérieur en France méditerranéenne. *C. R. Palevol* **6**, 301–309 (2007).
153. L. Slimak, D. Pesesse, Y. Giraud, Reconnaissance d'une installation du Protoaurignacien en vallée du Rhône. Implications sur nos connaissances concernant les premiers hommes modernes en France méditerranéenne. *C. R. Palevol* **5**, 909–917 (2006).
154. J. Zilhão, D. E. Angelucci, E. Badal-García, F. d'Errico, F. Daniel, L. Dayet, K. Douka, T. F. G. Higham, M. J. Martínez-Sánchez, R. Montes-Bernárdez, S. Murcia-Mascarós, C. Pérez-Sirvent, C. Roldán-García, M. Vanhaeren, V. Villaverde, R. Wood, J. Zapata, Symbolic use of marine shells and mineral pigments by Iberian neandertals. *Proc. Natl. Acad. Sci. U.S.A.* **107**, 1023–1028 (2010).
155. M. Peresani, I. Fiore, M. Gala, M. Romandini, A. Tagliacozzo, Late Neandertals and the intentional removal of feathers as evidenced from bird bone taphonomy at Fumane Cave 44 ky B.P., Italy. *Proc. Natl. Acad. Sci. U.S.A.* **108**, 3888–3893 (2011).
156. C. Finlayson, K. Brown, R. Blasco, J. Rosell, J. J. Negro, G. R. Bortolotti, G. Finlayson, A. Sánchez Marco, F. Giles Pacheco, J. Rodríguez Vidal, J. S. Carrión, D. A. Fa, J. M. Rodríguez Llanes, Birds of a feather: Neanderthal exploitation of raptors and corvids. *PLOS ONE* **7**, e45927 (2012).
157. A. Gómez-Olivencia, N. Sala, C. Núñez-Lahuerta, A. Sanchis, M. Arlegi, J. Rios-Garaizar, First data of Neandertal bird and carnivore exploitation in the Cantabrian Region (Axlor; Barandiaran excavations; Dima, Biscay, Northern Iberian Peninsula). *Sci. Rep.* **8**, 10551 (2018).
158. R. Blasco, J. Rosell, A. Sanchez-Marco, A. Gopher, R. Barkai, Feathers and food: Human-bird interactions at Middle Pleistocene Qesem Cave, Israel. *J. Hum. Evol.* **136**, 102653 (2019).
159. M. Romandini, M. Peresani, V. Laroulandie, L. Metz, A. Pastoors, M. Vaquero, L. Slimak, Convergent evidence of eagle talons used by late neanderthals in Europe: A further assessment on symbolism. *PLOS ONE* **9**, e101278 (2014).
160. D. Radovčić, A. Sršen, J. Radovčić, D. Frayer, Evidence for neandertal jewelry: Modified white-tailed eagle claws at krapina. *PLOS ONE* **10**, e0119802 (2015).
161. R. G. Klein, Out of Africa and the evolution of human behavior. *Evol. Anthropol.* **17**, 267–281 (2008).
162. A. M. Kubicka, Z. M. Rosin, P. Tryjanowski, E. Nelson, A systematic review of animal predation creating pierced shells: Implications for the archaeological record of the Old World. *PeerJ* **5**, e2903 (2017).
163. D. Garofoli, Do early body ornaments prove cognitive modernity? A critical analysis from situated cognition. *Phenomenol. Cogn. Sci.* **14**, 803–825 (2015).
164. W. Roebroeks, M. J. Sier, T. K. Nielsen, D. de Loecker, J. M. Pares, C. E. S. Arps, H. J. Mucher, Use of red ochre by early Neandertals. *Proc. Natl. Acad. Sci. U.S.A.* **109**, 1889–1894 (2012).
165. R. F. Rifkin, Assessing the efficacy of red ochre as a prehistoric hide tanning ingredient. *J. Afr. Archaeol.* **9**, 131–158 (2011).
166. P. R. B. Kozowyk, G. H. J. Langejans, J. A. Poulis, Lap shear and impact testing of ochre and beeswax in experimental Middle Stone Age compound adhesives. *PLOS ONE* **11**, e0150436 (2016).
167. S. Kadowaki, T. Kurozumi, H. Donald, Marine Shells from Tor Fawaz, Southern Jordan, and Their Implications for Behavioral Changes from the Middle to Upper Palaeolithic in the Levant, in *Learning Among Neanderthals and Palaeolithic Modern Humans*, Y. Nishiaki, O. Jöris, Eds. (Springer, 2019), pp 161–178.

168. J. F. Ewing, Preliminary note on the excavations at the Palaeolithic site of Ksâr 'Akil, Republic of Lebanon. *Antiquity* **21**, 186–196 (1947).
169. I. Azoury, F. R. Hodson, Comparing palaeolithic Assemblages: Ksar Akil, a Case Study. *World Archaeol.* **4**, 292–306 (1973).
170. K. Ohnuma, *Ksar Akil, Lebanon: A Technological Study of the Earlier Upper Palaeolithic Levels of Ksar Akil* (British Archaeological Reports International Series, 1988), vol. III: Levels XXV-XIV 338 pp.
171. C. A. Tryon, L. Metz, Archeological evidence for human dispersals around the Mediterranean basin? *Evol. Anthropol.* **28**, 233–235 (2019).
172. S. Kuhn, From Initial Upper Paleolithic to Ahmarian at Üçağızlı cave. *Anthropologie* **42**, 249–262 (2004).
173. S. L. Kuhn, M. C. Stiner, E. Güleç, I. Özer, H. Yılmaz, I. Baykara, A. Açıkkol, P. Goldberg, K. M. Molina, E. Ünay, F. Suata-Alpaslan, The early Upper Paleolithic occupations at Üçağızlı Cave (Hatay, Turkey). *J. Hum. Evol.* **56**, 87–113 (2009).
174. B. H. Smith, Patterns of molar wear in hunter-gatherers and agriculturalists. *Am. J. Phys. Anthropol.* **63**, 39–56 (1984).
175. C. G. Turner II, C. R. Nichol, G. R. Scott, Scoring procedures for key morphological traits of the permanent dentition: The Arizona State University Dental Anthropology System" in *Advances in Dental Anthropology*, M.A. Kelley, C.S. Larsen, Eds. (Wiley-Liss, 1991), pp. 13–31.
176. R. M. G. Martin, J.-J. Hublin, P. Gunz, M. M. Skinner, The morphology of the enamel-dentine junction in Neanderthal molars: Gross morphology, non-metric traits, and temporal trends. *J. Hum. Evol.* **103**, 20–44 (2017).
177. M. Martinón-Torres, M. M. de Pinillos, M. M. Skinner, L. Martín-Francés, A. Gracia-Téllez, I. Martínez, J. L. Arsuaga, J. M. B. de Castro, Talonid crests expression at the enamel–dentine junction of hominin lower permanent and deciduous molars. *C. R. Palevol* **13**, 223–234 (2014).
178. M. Buckley, M. Collins, J. Thomas-Oates, J. C. Wilson, Species identification by analysis of bone collagen using matrix-assisted laser desorption/ionisation time-of-flight mass spectrometry. *Rapid Commun. Mass Spectrom.* **23**, 3843–3854 (2009).
179. M. Pal Chowdhury, R. Wogelius, P. L. Manning, L. Metz, L. Slimak, M. Buckley, Collagen deamidation in archaeological bone as an assessment for relative decay rates. *Archaeometry* **61**, 1382–1398 (2019).
180. M. Buckley, R. A. Fariña, C. Lawless, P. S. Tambusso, L. Varela, A. A. Carlini, J. E. Powell, J. G. Martinez, Collagen sequence analysis of the extinct giant ground sloths *Lestodon* and *Megatherium*. *PLOS ONE* **10**, e0139611 (2015).
181. R. Fleischmajer, J. S. Perlish, R. E. Burgeson, F. Shaikh-Bahai, R. Timpl, Type I and type III collagen interactions during fibrillogenesis. *Ann. N. Y. Acad. Sci.* **580**, 161 (1990).
182. R. J. Wenstrup, J. B. Florer, E. W. Brunskill, S. M. Bell, I. Chervoneva, D. E. Birk, Type V collagen controls the initiation of collagen fibril assembly. *J. Biol. Chem.* **279**, 53331–53337 (2004).
183. A. Baker, P. L. Smart, R. L. Edwards, D. A. Richards, Annual growth banding in a cave stalagmite. *Nature* **364**, 518–520 (1993).
184. A. Baker, C. L. Smith, C. Jex, I. J. Fairchild, D. Genty, L. Fuller, Annually laminated speleothems: A review. *Int. J. Speleol.* **37**, 193–206 (2008).
185. M. S. Roberts, P. L. Smart, A. Baker, Annual trace element variations in a Holocene speleothem. *Earth Planet. Sci. Lett.* **154**, 217–246 (1998).
186. J.M. Desmarchelier, *High-resolution Palaeoenvironmental Information from Southeast Australian Speleothems.* PhD Thesis, University of Tasmania, Australia (1999).
187. Y. Huang, I. J. Fairchild, A. Borsato, S. Frisia, N. J. Cassidy, F. McDermott, C. J. Hawkesworth, Seasonal variations in Sr, Mg and P in modern speleothems (Grotta di Ernesto, Italy). *Chem. Geol.* **175**, 429–448 (2001).
188. I. J. Fairchild, A. Baker, A. Borsato, S. Frisia, R. W. Hinton, F. McDermott, A. F. Tooth, Annual to sub-annual resolution of multiple trace-element trends in speleothems. *J. Geol. Soc. Lond.* **158**, 831–841 (2001).
189. P. Treble, J. M. G. Shelley, J. Chappell, Comparison of high resolution sub-annual records of trace elements in a modern (1911–1992) speleothem with instrumental climate data from southwest Australia. *Earth Planet. Sci. Lett.* **216**, 141–153 (2003).
190. K. Johnson, C. Hu, N. Belshaw, G. Henderson, Seasonal trace-element and stable-isotope variations in a Chinese speleothem: The potential for high-resolution paleomonsoon reconstruction. *Earth Planet. Sci. Lett.* **244**, 394–407 (2006).
191. H. M. Stoll, W. Müller, M. Prieto, I-STAL, a model for interpretation of Mg/Ca, Sr/Ca and Ba/Ca variations in speleothems and its forward and inverse application on seasonal to millennial scales. *Geochem. Geophys. Geosyst.* **13**, 1–27 (2012).
192. G. Nagra, P. C. Treble, M. S. Andersen, P. Bajo, J. Hellstrom, A. Baker, Dating stalagmites in Mediterranean climates using annual trace element cycles. *Nat. Sci. Rep.* **7**, 1–12 (2017).
193. S. Vandevelde, J.-L. Lacour, C. Quéré, L. Marie, C. Petit, L. Slimak, Identification du rythme annuel de précipitation des carbonates pariétaux pour un calage micro-chronologique des occupations archéologiques pyrogéniques: Cas de la Grotte Mandrin (Malataverne, Drôme, France) [Identification of parietal carbonates' annual precipitation rate for a microchronological setting of pyrogenic archaeological occupations: The Grotte Mandrin (Malataverne, Drome, France) case]. *BSGF Earth Sci. Bull.* **192**, 1–22 (2021).
194. J. Durcan, G. King, G. Duller, DRAC: Dose rate and age calculator for trapped charge dating. *Quat. Geochronol.* **28**, 54–61 (2015).
195. S. W. Hillson, E. Trinkaus, Comparative Dental Crown Metrics, in *Portrait of the Artist as a Child. The Gravettian Human Skeleton from the Abrigo do Lagar Velho and its Archaeological Context*, J. Zilhão, E. Trinkaus (Instituto Português de Arqueologia, Lisboa, 2002), pp. 356–364.
196. E. Barberia, M. C. Suárez, G. Villalón, M. Maroto, F. García-Godoy, Standards for mesiodistal and buccolingual crown size and height of primary molars in a sample of Spanish children. *Eur. J. Paed. Dent.* **10**, 169–175 (2009).
197. NESPOS Database, Neanderthal Studies Professional Online Service. (2020).
198. ESRF Paleontological Microtomographic database (2020);http://paleo.esrf.eu.
199. P. Bayle, R. Macchiarelli, E. Trinkaus, C. Duarte, A. Mazurier, J. Zilhao, Dental maturational sequence and dental tissue proportions in the early Upper Paleolithic child from Abrigo do Lagar Velho, Portugal. *Proc. Natl. Acad. Sci. U.S.A.* **107**, 1338–1342 (2010).
200. M. Le Luyer, *Dental Evolution in Late Pleistocene and Early Holocene Human Populations (19000–5500 Cal. BP): A Whole Crown Perspective in the Aquitaine Basin, Southwest France, and Its Margins.* PhD Thesis, Université de Bordeaux, France (2016).
201. C. Zanolli, L. Bondioli, A. Coppa, C. M. Dean, P. Bayle, F. Candilio, S. Capuani, D. Dreossi, I. Fiore, D. W. Frayer, Y. Libsekal, L. Mancini, L. Rook, T. Medin Tekle, C. Tuniz, R. Macchiarelli, The late early Pleistocene human dental remains from Uadi Aalad and Mulhuli-Amo (Buia), Eritrean Danakil: Macromorphology and microstructure. *J. Hum. Evol.* **74**, 96–113 (2014).

Acknowledgments: We deeply acknowledge the Service Régional de l'Archéologie Auvergne Rhône-Alpes and the city of Malataverne that supported the 30 years of continuous field researches in Grotte Mandrin. We thank the many curators and colleagues who granted access to the comparative fossil and recent hominin specimens for scanning, as well as the online sharing platforms of the Nespos Society and ESRF Paleontological database (http://paleo.esrf.eu). We thank Harvard University's Peabody Museum of Archaeology and Ethnology for allowing access to the Ksar Akil collections by L.M. and L.S. For analytical support and microtomographic scanning and sharing of the material, we acknowledge B. Duployer and C. Tenailleau (University of Toulouse); A. Mazurier and R. Macchiarelli (University of Poitiers); M. Honegger (University of Neuchâtel); F. Bon and J. Cauliez (University of Toulouse J. Jaurès); S. Hérouin (Archeological Service of Chartres); R. Lebrun (University of Montpellier); A. Bravin, C. Nemoz, and P. Tafforeau (ESRF Synchrotron); P. Bayle, I. Crevecoeur, R. Ledevin, M. Matu, S. Rottier, and F. Santos (University of Bordeaux); and M. Le Luyer (University of Kent). **Funding:** Long-term research was supported by the Service Régional de l'Archéologie Auvergne Rhône-Alpes, the French CNRS, and the city of Malataverne. Three-dimensional site models were granted by the city of Malataverne and the Auvergne Rhône-Alpes region. This project received funding from the European Research Council (ERC) under the European Union's Horizon 2020 research and innovation program (grant agreement no. 681605) and the Seventh Framework Program (FP7/2007-2013)/ERC grant no. 324139 ("PalaeoChron") awarded to T.H. Research of C.S. is supported by the Calleva Foundation and the Human Origins Research Fund. Research on Ksar Akil was supported by a Fyssen Foundation grant awarded to L.M., by CNRS funds (Aide à la Mobilité Internationale) awarded to L.S., and the Radcliffe Institute for Advanced Study at Harvard University awarded to L.M. Fuliginochronological research was granted by the L'Oréal-UNESCO Foundation FWIS awarded to S.V. and by Université Paris 1–Panthéon-Sorbonne funds (Aide de l'ED112) awarded to S.V. Luminescence dating research conducted by M.D. and L.A. was supported by Australian Research Council Future Fellowship grant FT200100816. Scanning and analysis of the comparative material were funded by the LabEx DHP (LaScArBx-AAP1-2011), the ANR Big Dry (ANR-14-CE31), and the LabEx Djibouti (LaScArBx-AAP5-2015). This study also received financial support from the French government in the framework of the University of Bordeaux's IdEx "Investments for the Future" program/GPR Human Past. **Author contributions:** L.S. and L.M. excavated the site and led the scientific project. Microtomographic-based data were collected and analyzed by C.Z. L.S. analyzed the lithic technical systems. Spatial analyses were performed by P.Y. and X.M. Radiometric and luminescence dating analyses and Bayesian age modeling were performed by T.H., M.F., J-L.S., L.J.A., M.D., K.D., N.M., G.G., and H.V. Fuliginochronological analyses were realized by S.V. Ancient DNA analyses were performed by A.S.-O. and L.O. L.S., C.Z., L.M., and J.E.L. wrote the manuscript with contributions from all other authors. **Competing interests:** The authors declare that they have no competing interests. **Data and materials availability:** All data needed to evaluate the conclusions in the paper are present in the paper and/or the Supplementary Materials.

Submitted 11 June 2021
Accepted 19 November 2021
Published 9 February 2022
10.1126/sciadv.abj9496

ScienceAdvances

Modern human incursion into Neanderthal territories 54,000 years ago at Mandrin, France

Ludovic SlimakClément ZanolliTom HighamMarine FrouinJean-Luc SchwenningerLee J. ArnoldMartina DemuroKaterina DoukaNorbert MercierGilles GuérinHélène ValladasPascale YvorraYves GiraudAndaine Seguin-OrlandoLudovic OrlandoJason E. LewisXavier MuthHubert CamusSégolène VandeveldeMike BuckleyCarolina MallolChris StringerLaure Metz

Sci. Adv., 8 (6), eabj9496.